Precambrian Research 224 (2013) 268–286

Contents lists available at SciVerse ScienceDirect

Precambrian Research

journal homepage: www.elsevier.com/locate/precamres

Geochronological constraints on the magmatic and tectonic development of the Pongola Supergroup (Central Region), South Africa

Samuel B. Mukasa[a,1], Allan H. Wilson[b,*], Katherine R. Young[c,2]

[a] Department of Earth Science, University of New Hampshire, 214 James Hall, 56 College Road, Durham, NH 03824, United States
[b] School of Geosciences, University of the Witwatersrand, 2050 Wits, South Africa
[c] Department of Earth and Environmental Sciences, University of Michigan; 2534C.C. Little Bldg., 425 E. University Ave., Ann Arbor, MI 48109-1063, United States

ARTICLE INFO

Article history:
Received 13 December 2011
Received in revised form 26 August 2012
Accepted 4 September 2012
Available online xxx

Keywords:
Archean tectonics
Pongola
Kaapvaal Craton
U–Pb geochronology
A-type granite

ABSTRACT

The Pongola Supergroup, located at the southeast margin of the Kaapvaal Craton, is a well-preserved Meso-Archean volcano-sedimentary sequence containing the full spectrum of basalt–andesite–dacite–rhyolite volcanic rocks, emplaced on 3.1–3.3 Ga crystalline basement rocks. We have carried out a zircon U–Pb dating study using high resolution, secondary ionization mass spectrometry (SIMS) on volcanic layers at various levels in the lava flow successions, and on the post-Pongola granitoids emplaced in the immediate vicinity of the Pongola Supergroup, with the primary aim of determining volcanic eruption rates, Archean crustal dynamics, and the tectonic setting of the lavas and granitoids. The pre-Pongola Tsawela Gneiss on the northeastern side of the Pongola basin gives an age of 3428 ± 22 Ma, consistent with other determinations in this area. Crystallization ages of the granitoids and gneisses in the southwest appear to be generally younger at 3.1–3.2 Ga, indicating the presence of contrasting crustal blocks on each side of the Pongola depositary. However, the greenstone fragments on the southwest side are 3.5–3.3 Ga in age indicating a complex history. U–Pb zircon dates set the oldest Pongola volcanic layer in the Nsuze Group at 2980 ± 10 Ma and the uppermost layer contained within the mainly sedimentary Mozaan Group at 2954 ± 9 Ma. These dates provide the first direct estimate of the period of deposition for the Pongola sequence. Xenocrystic zircons in post-Pongola granitoid intrusions have inherited cores with ages similar to those of the Pongola volcanic rocks, and have younger emplacement ages between 2837 ± 6 Ma and 2717 ± 11 Ma. ε_{Nd} values range from -2.55 for basalt to -4.20 for rhyolite in the Pongola volcanic suite, whereas post-Pongola granitoids have ε_{Nd} values ranging from -2.08 to -6.14. This indicates that all rock types, including the basalts, have some contribution from crustal melts or aged enriched mantle lithospheric materials. Although trace element distributions for these rocks show characteristics similar to those of modern arcs, including negative anomalies in Th, Ta, Nb, Ce, and P, these may have been inherited from previously formed crust and may not be indicative of the Pongola tectonic environment. Evidence of rapid deposition, a preponderance of intermediate lavas, discordance of bounding crustal blocks and consistent structural trends in the area, are similar to features found in continental arc basins currently observed in the southwestern USA, and may present an alternative model to those currently accepted for Archean terranes in early-formed cratons.

The age determinations of the post-Pongola granitoid intrusions indicate crustal recycling on a short time scale during the Archean. The post-Pongola granitoids are classic A-type granites with strongly elevated REE patterns, deep Eu/Eu* anomalies, high Fe/Mg ratios and highly elevated HFSE contents, and are possibly the oldest occurrence of this class of granitiod rocks representing the complete and final stage of development of the world's oldest stabilized Archean craton.

1. Introduction

Much of the continental crust that formed during Archean time has been reworked and recycled by later tectonic events and much of what remains has been metamorphosed, making it difficult to determine how the crust formed. Many Archean supracrustal rock suites within the Zimbabwe and Kaapvaal Cratons of southern Africa, including the Pongola Supergroup (the subject of this study), have relatively well-preserved primary structures and geochemical

* Corresponding author. Tel.: +27 11 7176564; fax: +27 11 717 6579.
E-mail address: Allan.Wilson@wits.ac.za (A.H. Wilson).
[1] Tel.: +1 (603) 862 1781.
[2] Tel: +1 (734) 647 5533.

0301-9268/$ – see front matter
http://dx.doi.org/10.1016/j.precamres.2012.09.015

signatures which may be used to place constraints on the tectonic setting and genetic relationships of the rocks, thereby contributing to our understanding of crust-forming processes during the Archean. A further important issue is how magmatic rock suites of widely contrasting compositions, as observed in the Pongola Supergroup and the pre- and post- Pongola granitoids, are related to each other tectonically, structurally and geochemically.

The purpose of this study is to provide new data on the crystallization ages of the Nsuze and Mozaan Groups and associated pre- and post-Pongola granitoids in the immediate vicinity in the north-central part of the Pongola basin in order to assess the tectonic and magmatic relationship of these rocks within the general setting of the eastern Kaapvaal Craton.

The Pongola Supergroup is situated in the southeastern sector of the Kaapvaal Craton (Fig. 1A) and extends as a broadly north–south trending linear belt over a distance of 250 km. The area of study is the north-central region where the Pongola Supergroup extends into northern Mpumalanga Province, South Africa, and southwestern Swaziland. In this area, mafic to silicic volcanic rocks and sediments were deposited on basement granitoids, gneisses and early Archean greenstone belt remnants, some intensely sheared and metamorphosed (Armstrong et al., 1982, 1986). The high proportion of silicic and intermediate compositions (andesite) of the volcanic rocks, and the relative lack of deformation of the Pongola Supergroup in the area of interest, contrast with typical greenstone belts elsewhere of the same approximate age in southern Africa and are thus significant in understanding the development of stable crust in the Archean. The geochronology presented here focuses on the central part of the Mesoarchean Pongola Supergroup, and aimed to evaluate new high-precision zircon U–Pb ages in terms of the known compositions of the volcanic rocks to further understand the tectonic setting of this volcanism.

The tectonic setting of many Archean terrains remains highly controversial although granite–greenstone associations in some areas of the world are unequivocally arc-like in character (Thurston, 1994), and particularly in the late-Archean. Arc-like geochemical signatures for the Superior Province include calc-alkaline trends for major elements, trace element distributions characterized by light REE enrichment, and negative Ti, Nb, and Ta anomalies on primitive mantle-normalized element distribution plots (Hallberg et al., 1976; Capdevila et al., 1982; Gaal, 1986; Sylvester et al., 1987; Kusky, 1990). However, these geochemical characteristics are also the signature of crustal contamination. In spite of the apparent evidence to support plate tectonic processes in the Archean, strong counter arguments exist including the superficial resemblance of geochemical characteristics between modern arc lavas and some Archean ones (Bédard et al., 2012). It is only seldom that litho-tectonic assemblages are preserved well enough in Archean terranes to invite comparison to the rock suites observed in typical magmatic arcs (Hamilton, 1998; Bédard et al., 2012). The Pongola Supergroup is a thick, relatively undeformed supracrustal sequence of volcanic and sedimentary rocks that was emplaced at a time (c.3 Ga) when in most parts of the Earth the dominant processes resulted in highly deformed greenstone belts. The Pongola Supergroup therefore must be viewed in the context that it is an integral part of the Kaapvaal Craton that was stabilized earlier than almost all other terranes on the planet and therefore may have been subject to tectonic processes in this period of Earth's history that only appeared several hundred million years later in other areas. The presentation of further precise geochronological and geochemical data contributes to the understanding of this possibly unique environment.

Based on structural and field evidence, it has been previously suggested that the Pongola volcanic rocks were emplaced in a continental rift environment (Burke et al., 1985; McCourt, 1995; Gold and Von Veh, 1995), but the nature of the volcanism and the compositions are dissimilar to those that characterize modern-day settings of this type. Geochemical evidence presented by Armstrong et al. (1986) suggested a broadly continental setting but the precise nature of the tectonic setting for the Pongola Supergroup remains uncertain.

For this study, we have selected samples of critical rock types to carry out precise SIMS U–Pb isotopic measurements on zircons combined with Nd model ages, together with major and trace element compositions for the sample set that includes pre-Pongola basement granitoid rocks, volcanic rocks of the Pongola Supergroup and post-Pongola granitoids. The objectives of the work are to present the new geochronological data in the context of existing ages and to place constraints on the tectonic setting and emplacement history of the Pongola Supergroup depository in this area of the Kaapvaal Craton. The zircon U–Pb isotopic determinations presented here are in most cases based on replicate analyses of grains, with good agreement among them, giving confidence about the robustness of the ages.

2. Geologic setting

The eastern part of the Kaapvaal Craton in eastern South Africa and southeast Swaziland records an unbroken geological history from 3.6 Ga in the Ancient Gneiss Complex (AGC), ostensibly the basement to the Barberton Greenstone Belt (3.5 Ga), through to post-Barberton orogenic processes, including the development of a putative volcanic arc and suture zone (Lowe, 1999; Kisters et al., 2006; Stevens and Moyen, 2007; Hunter and Wilson, 1988) and stabilization of the Craton prior to deposition of the extensive volcanic rocks and sediments of the Pongola Supergroup at approximately 3 Ga. Post-Pongola granitoids were emplaced at 2.8–2.7 Ga. Reconstruction of these tectonic events is slowly taking shape, aided in part by new high-precision geochronology. A main contribution of this paper is new ages of volcanic rocks of the Pongola Supergroup as well as of the pre- and post-Pongola terranes in the rocks adjacent to the Pongola depository.

2.1. *Terminology and summary of sequence of events in the Kaapvaal Craton in south west Swaziland and eastern South Africa*

The Archean geology of SW Swaziland (Wilson, 1982) and central eastern South Africa (Fig. 1A) is important in the setting of the Pongola Supergroup both from the aspects of the pre-Pongola basement and post-Pongola magmatic activity. The various granitiod bodies that occur in southeast South Africa and southwest Swaziland are shown on the map in Fig. 1B and a summary of ages is given in Table 1. The oldest rocks in the Kaapvaal Craton are the bimodal gneisses of the Ancient Gneiss Complex (AGC) (Hunter, 1973) and the Ngwane Gneiss that comprise the basement to the Barberton greenstone belt. Intrusions into the Ngwane Gneiss of hornblende tonalite, known as the Tsawela and Mhlatuzane Gneisses preceded greenstone belt formation. The Mahamba Gneiss is a semi-pelitic garnetiferous gneiss of uncertain age, initially considered to equate with the Ngwane Gneiss, but is likely to be younger than the early gneissic phases (Wilson, 1982). Late Paleo-Archean trondhjemites, called the Usutu Suite, intruded the earlier gneisses but components of this body represent a distinct 3.2 Ga event (Schoene and Bowring, 2010) together with enclaves of 3.56 Ga Ancient Gneiss Complex (Kröner, 2007). This was followed by the extensive sheet-like granodioritic suite of the 3.1 Ga Mpuluzi intrusion (previously known as the Lochiel Granite) forming the basement to the Pongola rocks in their most northerly occurrence.

The dominantly volcanic (in the northern region) and essentially undeformed Nsuze Group formed the basal unit of the Pongola Supergroup followed by the extensive, and dominantly

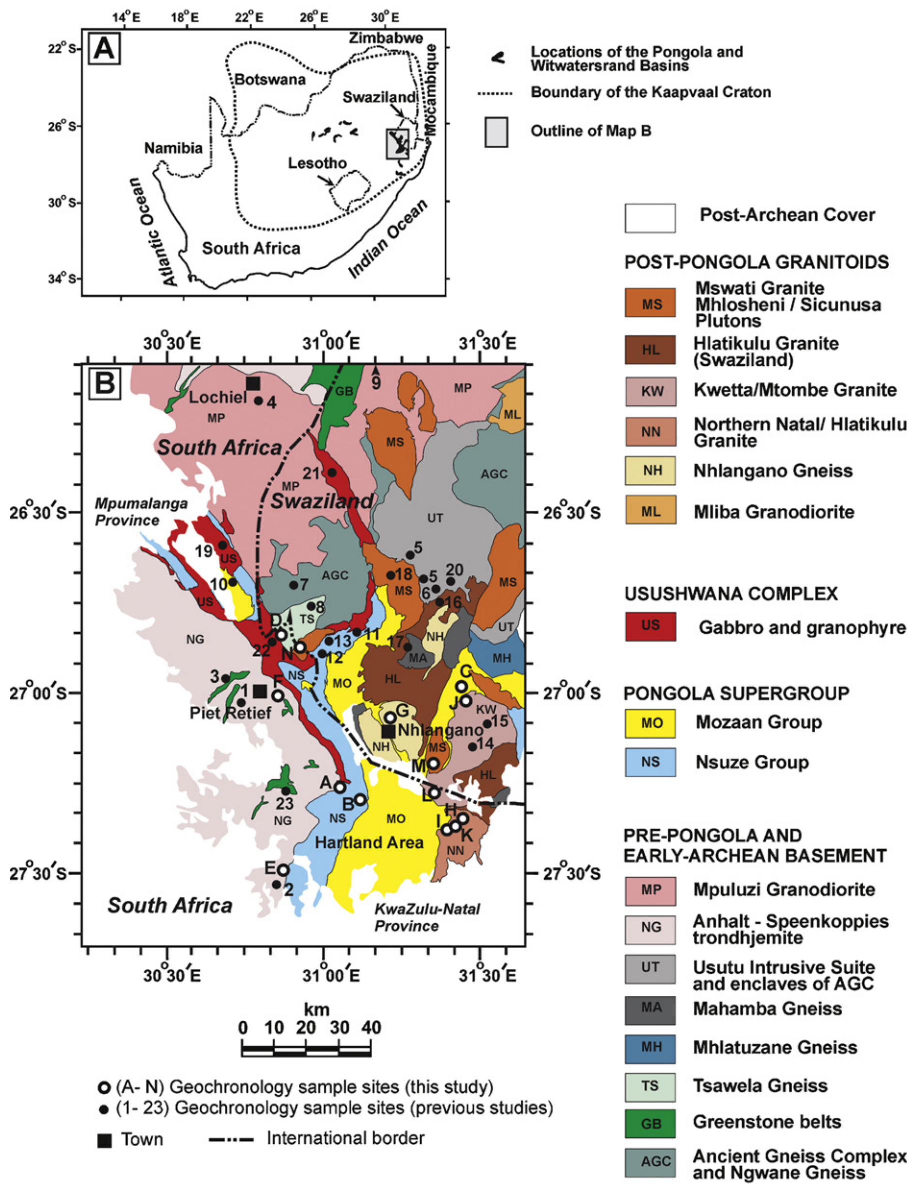

Fig. 1. (A) General location and setting of the Meso-Archean Pongola and Witwatersrand basins in relation to the Kaapvaal Craton in southern Africa. (B) General geology of the Pongola area showing the volcanic rocks as well as the pre-Pongola and post-Pongola granitoids in eastern Mpumalanga and Swaziland. Swaziland map modified from Wilson (1982). Open circles show locations of samples in this study (Exact locations and sample descriptions are given in the Supplementary Data File): (A) CG-170 Nsuze basalt, (B) CG-171 Nsuze rhyolite, (C) CG-174 Mozaan andesite, (D) CG-65 Tsawela Gneiss, (E) CG-73 Anhalt granite, (F) PG-36 Anhalt granite, (G) Nhlangano gneiss CG-172, (H) Northern Natal/Hlatikulu granite PG-44, (I) Northern Natal/Hlatikulu granite PG-45, (J) Kweta Granite CG-175, (K) Northern Natal Granite PG-46, (L) Kweta Granite PG-49, (M) Mswati Granite CG-173, (N) Mswati Granite CG-66. Localities of sites of previous studies are as follows (Localities are noted by numbers and correspond to those given in Table 1): 1. Anhalt granite (Saha et al., 2010); 2. Natal Spa granite (Meyer et al., 1993); 3. Anhalt leucotonalite (Farrow et al., 1990); 4. Mpuluzi Granite (Kamo and Davis, 1994); 5. Usutu granitoid suite (Schoene and Bowring, 2010); 6. Nhlangano/Mahamba gneiss (Schoene and Bowring, 2010); 7. Ancient Gneiss Complex (Carlson et al., 1983); 8. Tsawela Gneiss (Kröner et al., 1989); 8. Tsawela Gneiss (Kröner and Tegtmeyer, 1994); 9. Ngwane Gneiss (Compston and Kröner, 1988); 10. Mozaan Group (Walraven and Pape, 1994); 11. Nsuze Group (Hegner et al., 1984); 12. Nsuze Group (Nhleko, 2003); 13. Nsuze Group (Hegner et al., 1994); 14. Kwetta Granite (Meyer et al., 1993); 15. Kwetta Granite (Maphalala and Kröner, 1993); 16 and 17. Hlatikulu granite (Schoene and Bowring, 2010); 18. Mswati Granite (Maphalala and Kröner, 1993); 19. Mafic rock and granophyre (Hegner et al., 1994); 20. Tonalitic gneiss in the Ngwempisi River (Kröner, 2007); 21. Usushwana gabbro east limb (Olsson, 2012); 22. Usushwana gabbro west limb (Olsson, 2012); 23. Peridotite of the Commondale greenstone belt (Wilson and Carlson, 1989).

sedimentary, Mozaan Group. Rocks of both the Nsuze and Mozaan Groups were intruded by the mafic Usushwana Complex. Although an age of 2871 ± 30 is accepted for emplacement of this complex, recent SHRIMP analyses have yielded significantly older ages Olsson (2012) (Table 1). On mainly structural grounds, the Mlibi granodiorite is recognized to be the first phase of the post-Pongola intrusions, followed by the Nhlangano gneiss dome complex. The Kwetta and Mtombe granitoid bodies are rapakivi granites of broad dome-like form that extend into South Africa. The intrusion of the wide-spread late-Archean Hlatikulu granite (also extending into South Africa) (Fig. 1B) caused local deformation of the Mozaan Group and was followed by the Mswati/Mlosheni granitoid bodies as sharply transgressive anorogenic plutons representing the final intrusive phase.

Convergent margins and strike-slip boundaries can juxtapose rocks of different origins, ages and chemical and isotopic signatures. Hunter et al. (1983) reported that the granodiorites on the southwestern side are similar in mineralogy to the Mpuluzi sheet granitoid on the northeastern side of the depository. Previously determined ages, and supported by the new age determinations of this work, emphasize the generally older ages to the east and northeast of the Pongola basin, whereas younger c.3.1–3.2 Ga terrane

Table 1
Summary of reported ages for the Pongola Supergroup and pre- and post-Pongola granitoids and selected greenstones.

Unit	Age (Ma)	Method	Reference
Pre-Pongola granitoids			
South West side (including greenstones):			
G4 Granite	3163 ± 103	Rb–Sr whole rock isochron	Allsopp (1961)
Anhalt granite (1)	3193 ± 8	U–Pb SHRIMP	Saha et al. (2010)
Anhalt trondhjemite (1)	3222 ± 8	U–Pb SHRIMP	Saha et al. (2010)
Natal Spa granite (2)	3223 ± 2	U–Pb single zircon	Meyer et al. (1993)
Anhalt leucotonalite (Piet Retief) (3)	3250 ± 39	Rb–Sr whole rock isochron	Farrow et al. (1990)
Commondale greenstones (23)	3316 ± 16	Sm–Nd whole rock isochron	Wilson and Carlson (1989)
Nondweni greenstones	3418 ± 5	U–Pb SHRIMP	Xie et al. (2012)
Nondweni greenstones	3532 ± 4	U–Pb SHRIMP	Xie et al. (2012)
Nondweni greenstones	3520 ± 6	U–Pb SHRIMP	Xie et al. (2012)
North East side:			
Mpuluzi Granite (4)	3107 + 4/−2	U–Pb zircon/Titante	Kamo and Davis (1994)
Usutu granitoid suite (5)	3221.6 ± 0.5	U–Pb zircon	Schoene and Bowring (2010)
Usutu granitoid suite (5)	3236.1 ± 0.5	U–Pb zircon	Schoene and Bowring (2010)
Usutu granitoid suite (6)[a]	3265.5 ± 0.5	U–Pb zircon	Schoene and Bowring (2010)
AGC, including Tsawela Gneiss (7)	3417 ± 34	Sm–Nd whole rock isochron	Carlson et al. (1983)
Tsawela Gneiss (8)	3436 ± 6	Pb–Pb single zircon evaporation	Kröner and Tegtmeyer (1994)
Tsawela Gneiss (8)	3458 ± 6	Pb–Pb evaporation	Kröner et al. (1989)
Ngwane Gneiss AGC (9)	3644 ± 2	U–Pb SHRIMP	Compston and Kröner (1988)
Tonalite gneiss AGC (20)	3563 ± 3	U–Pb SHRIMP	Kröner (2007)
Pongola and Usushwana Complex			
Qtz Porphyry Sill (Mozaan Group SE Swaziland – Minimum age)	2837 ± 4.7	U–Pb zircon SHRIMP	Gutzmer et al. (1999)
Mozaan (10)	2860 ± 26	Pb–Pb whole rock errorchron age (Mozaan)	Walraven and Pape (1994)
Nsuze (11)	2883 ± 69	Rb–Sr whole rock age (reset?)	Hegner et al. (1984)
Nsuze (11)	2934 ± 114	Sm–Nd whole rock isochron from basalt-rhyolite suite	Hegner et al. (1984)
Nsuze (11)	2940 ± 22	U–Pb zircon concordia intercept	Hegner et al. (1984)
Nsuze (12)	2977 ± 5	U–Pb zircon SHRIMP	Nhleko (2003)
Nsuze (13)	2985 ± 1	U–Pb (abraded) zircon evaporation age	Hegner et al. (1994)
Usushwana Complex (21)	2989.2 ± 0.8	U–Pb Baddeleyite (ID-TIMS)	Olsson (2012)
Usushwana Complex (22)	2989.8 ± 1.7	U–Pb Baddeleyite (ID-TIMS)	Olsson (2012)
Nsuze	3083 ± 150	Rb–Sr whole rock isochron	Burger and Coertze (1973)
Nsuze	3090 ± 90	U–Pb from zircons	Burger and Coertze (1973)
Post-Pongola			
Usushwana Complex (Reset age)	2386 ± 58	$^{40}Ar/^{39}Ar$	Layer et al. (1988)
Nhlangano	2244 ± 355	Rb–Sr whole rock isochron	Barton et al. (1983)
Mswati (Mshlosheni)	2286 ± 304	Rb–Sr whole rock isochron	Barton et al. (1983)
Hlatikulu	2417 ± 148	Rb–Sr whole rock isochron	Barton et al. (1983)
Kwetta	2520 ± 422	Rb–Sr whole rock isochron	Barton et al. (1983)
Kwetta (14)	2671 ± 3	Single zircon	Meyer et al. (1993)
Kwetta (15)	2722 ± 6	Pb–Pb zircon evaporation	Maphalala and Kröner (1993)
Hlatikulu granite (16)	2728.9 ± 0.5	U–Pb zircon	Schoene and Bowring (2010)
Hlatikulu granite (17)	2729.8 ± 0.4	U–Pb zircon	Schoene and Bowring (2010)
Mswati (Mooihoek) (18)	2824 ± 6	Pb–Pb single zircon evaporation	Maphalala and Kröner (1993)
Usushwana Complex (19)	2871 ± 30	Sm–Nd whole rock	Hegner et al. (1984)
Usushwana Complex	2875 ± 40	Rb–Sr whole rock and Sm–Nd mineral	Layer et al. (1988)

Numbers in brackets refer to localities given in Fig. 1. Where no reference is given to the locality this implies that the locality area is outside that represented in Fig. 1. Localities of sites having Rb–Sr ages with large errors are not shown in Fig. 1.
The most recent determined ages on the Usushwana Complex are listed with those of the Nsuze volcanic rocks to emphasize the similarity in ages with the oldest ages obtained for the lavas. Ages presented for the Usushwana Complex (Olsson, 2012) from thesis material are by permission of the author.
[a] Incorrectly referred to as the Nhlangano gneiss in Schoene and Bowring (2010) in Fig. 10 of that work, whereas shown as part of the Usutu suite in Fig. 6 and also in Wilson (1982).

denominates the southwestern area. Remnants of older greenstone belts of 3.4–3.3 Ga age (Wilson and Carlson, 1989; Xie et al., 2012) (Fig. 1B) indicate a protracted geological history with independent evidence of a widespread metamorphic event at c. 3.2 Ga in the southwestern terrane (Saha et al., 2010; Xie et al., 2010). The contrast in the crustal blocks, separated by the Pongola Supergroup, indicates the possibility of a wide-scale tectonic control extending over the period of emplacement of the pre-Pongola terrane, the Pongola basin itself, and the post-Pongola granitoids. The development of the Pongola Supergroup may possibly be attributed to a zone of weakness between contrasting crustal blocks. The post-Pongola granitoid bodies are exclusively located east of the Pongola volcano-sedimentary depository (Fig. 1B).

2.2. The structure of the Pongola Supergroup

The Pongola Supergroup in the central and northern regions varies from having almost no deformation, other than overall dipping at 20–35° to the east, and low grade metamorphism, to zones of intense deformation and metamorphic grade as high as granulite facies in Swaziland. Gold and Von Veh (1995) described a series of north and north-westerly structural trends with shear zones and thrust faults, also recognized by Matthews (1990), and parallel open style anticlines and synclines most clearly seen in the Hartland area (Fig. 1B). The northward trending Mahamba Shear Zone is a major zone of attenuation located SE of Piet Retief (Hunter and Wilson, 1988). Bounding shear zones are observed in the central Hartland area, and in the north where rocks of the Pongola Supergroup are juxtaposed with the Usushwana Complex as rifted boundaries to the basin, but deposition was not in a regional continental rift setting, as suggested by Burke et al. (1985).

2.3. Pre-Pongola granitoids

Previous studies (Hunter et al., 1984; Armstrong et al., 1986; Gold and Von Veh, 1995) referred to the granitoid basement rocks that bound the Pongola Supergroup in SW Swaziland and mid-eastern South Africa as the pre-Pongola granitoids (Fig. 1B and Table 1). More specifically, the granodiorites and migmatites to the north are collectively referred to as the Heerenveen, Mpuluzi and Piggs Peak Batholiths (Barton et al., 1983). The Ancient Gneiss Complex, the oldest crustal terrane extensively developed in central Swaziland (Hunter, 1973) borders the Nsuze Group to the northeast of the Pongola Supergroup (Fig. 1B) and comprises gneisses interlayered with amphibolites, dated at 3.6–3.2 Ga (Kröner and Tegtmeyer, 1994). Field evidence in Swaziland indicates that the AGC formed the basement to the eastern part of the Barberton Supergroup (Barberton Greenstone Belt) (Brandl et al., 2006).

Granitoid rocks of a variety of ages, and becoming increasingly well constrained as new age data is published, abut the volcanic rocks along the entire length of the Pongola basin (S. African Geol. Survey Map Number 2730, 1988). Recently some of these granitoid terranes have been mapped and characterized in detail (e.g., Schoene and Bowring, 2010). Hunter et al. (1984) and Farrow et al. (1990) observed these basement rocks as granodioritic, pegmatitic, gneissic and tabular leucotonalitic granites. Meyer et al. (1993) refer to the Mfule Gorge and Natal Spa tonalitic to trondhjemitic gneisses in the area, (the same gneissic granites discussed by Hunter et al. (1984)) but referred to in that work as the Anhalt trondhjemite suite (Fig. 1B).

Recent studies in Meso-Archean terranes have consolidated models for the development of the granitoids in the eastern Kaapvaal Craton following stabilization of the post-Barberton Greenstone Belt terranes (Schoene et al., 2008) as well as recognition of Meso-Archaean subduction processes following the deposition of the Onverwacht and Figtree Groups of the Barberton Supergroup (Moyen et al., 2007). Recent studies have also focused on the complex metamorphic history of the area (e.g., Saha et al. (2010) on the South African side and references therein) and provided additional new ages.

2.4. Pongola Supergroup

The Pongola Supergroup comprises a thick sequence of volcanic and sedimentary rocks located in the Mpumalanga and northern KwaZulu-Natal Provinces of South Africa and in Swaziland (Fig. 1A and B). The rocks in the northern and central areas crop out for about 120 km along the border between, and also within, the two countries dipping to the southeast at 26–78°. The Pongola Supergroup is divided into two units: the lower volcano-sedimentary Nsuze Group and upper, predominantly sedimentary Mozaan Group (Fig. 2) (Tankard et al., 1982; Hunter and Wilson, 1988; Beukes and Cairncross, 1991). The most striking feature of the Nsuze Group is its range of volcanic rock compositions spanning basalt to rhyolite, all volumetrically significant. Although such ranges in composition are observed in volcanic cycles in the Neo-Archean greenstones belts of the Superior Province (Canada) and Zimbabwe Craton, and in the early Archean sequences in the Pilbara (Van Kranendonk et al., 2007; Smithies et al., 2007), the proportion of andesite and rhyolite in the Pongola Supergroup is in comparison significantly greater and therefore atypical of Archean volcanism (Armstrong et al., 1982; Thurston, 1994).

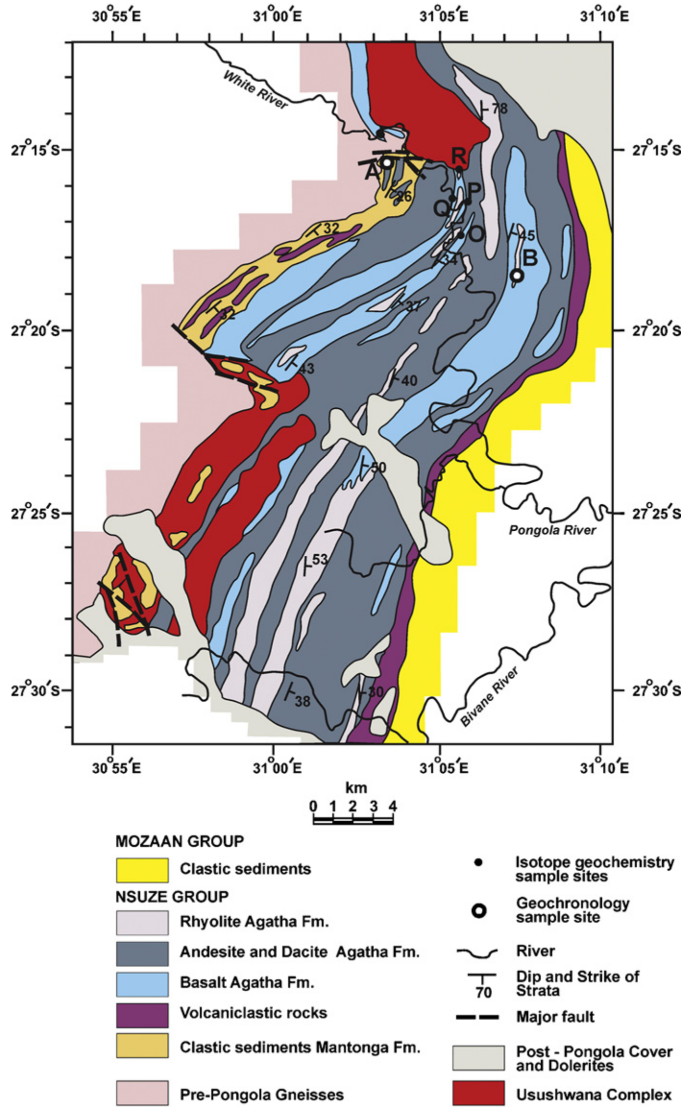

Fig. 2. Simplified geological map of the central area of the Nsuze Group showing distribution of basalts, andesites, dacites and rhyolites. Modified from mapping of Armstrong et al. (1982). Localities of samples used for geochronology: A. Andesite from the bottom of the Nsuze Group (CG-170); B. Rhyolite from the middle of the Nsuze Group (CG-171). The locality of the third sample (CG-174) used for U–Pb geochronology is shown as C in Fig. 1B. Samples used for isotope geochemistry of the Pongola lavas: O. Basalt (CG-22); P. Basaltic andesite tuff (PG-24); Q. Basaltic andesite lava (PG-26); R. Porphyritic rhyolite (CG-9).

In its most northerly exposures the base of the Nsuze Group is a thin quartz arenite, and locally conglomeratic unit that lies unconformably on the pre-Pongola granitoid basement rocks. Gold (2006) gives the thickness of the Nsuze Group in the Hartland area as 4600 m of dominantly volcanic rocks consisting mainly of basaltic andesite or andesite with relatively thin basalt, rhyolite, dacite and tuffaceous layers (Fig. 2). Two samples were used for age determinations, one from near the base of the succession and the second from near the top of Nsuze Group (Fig. 1B). Exact localities and rock descriptions of the samples shown in Figs. 1B and 2 are given in the electronic supplementary data file entitled ‘Sample Locations and Descriptions’. Other samples were used for Nd isotopic studies and are shown in Fig. 2. Estimates of the thickness of the Nsuze Group vary greatly because of facies variations from north to south and range from 4600 m to 9000 m (Kent, 1980; Armstrong et al., 1982; Burke et al., 1985; Wronkiewicz and Condie, 1989).

Although welded tuffs, vesicles, and intercalated lenses of fluvial sediments indicate mainly subaerial deposition, local pillow structures suggest subaqueous settings for some periods (Armstrong et al., 1986; Wilson and Grant, 2006). The top of the Nsuze Group is marked by an intercalation of volcanogenic and sedimentary rocks. The dominantly sedimentary Mozaan Group (4800 m thick in the Hartland area (Gold, 2006)), unconformably overlies the Nsuze Group, and is made up primarily of sandstone, shale, mudstone, and locally developed banded iron formations with thin, interbedded layers of volcanic rocks towards the top of the succession (Beukes and Cairncross, 1991). Locally, stromatolite-bearing carbonates are also present in the southern region indicating shallow marine environments and deposition (Von Brunn and Hobday, 1976; Beukes and Lowe, 1989; Hicks et al., 2011).

2.5. Post-Pongola granitoids

A number of intrusive felsic stocks crop out in close temporal and spatial association with the Mozaan Group of the Pongola Supergroup in southern Swaziland and the northern Mpumalanga Province of South Africa and are known as the post-Pongola granitoids. These include the Mswati granitoid suite (Fig. 1B; with individual plutons known as Mbabane, Sinceni, Mhlosheni and Mooihoek), Hlatikulu granite and the Kwetta/Mtombe granites. Petrographic characteristics of each of these plutons are given on the geologic map of Swaziland (Wilson, 1982), and in general, all are medium- to coarse-grained, igneous textured granites with supposed calc-alkaline geochemical characteristics. The Nhlangano pluton is gneissic in character and recognized on structural grounds as being the oldest of the post-Pongola intrusions (Hunter, 1957), a conjecture supported by the chronological studies presented here. Further detailed structural observations have been reported by Schoene and Bowring (2010). The exact link of these granitoids with rocks of the Pongola Supergroup remains unclear. Through precise age determinations and geochemical characterization of this study we attempt to provide insight into their emplacement history and origin.

3. Previous geochronological studies

3.1. Pre-Pongola basement rocks in the vicinity of the Pongola Basin

The Tsawela, Mhlatuzane and the Ngwane Gneisses comprise the basement to the Barberton Greenstone Belt and are constrained to minimum ages of $3467 + 12/-7$ Ma and 3458 ± 8 Ma (Kamo et al., 1990; Kamo and Davis, 1991; Kamo and Davis, 1994). Armstrong et al. (1990) obtained an age of 3472 ± 5 on zircons from interflow sediments in the Komati Formation of the Barberton greenstone belt and this defines the maximum age for the basal Komati Formation. Ages for the Tsawela Gneiss range from 3458–3417 Ma (see Table 1 for summary and references) and Compston and Kröner (1988) obtained an age of 3644 ± 2 on the Ngwane Gneiss component of the AGC. Kröner (2007) presents an age of 3563 ± 3 for a tonalitic gneiss in the Ngwenpisi River in west central Sawziland (Table 1; Fig. 1B).

Migmatitic granodiorite and granite of the Mpuluzi Batholith (Fig. 1B) gave an age of $3107 + 4/-2$ Ma (U–Pb zircon/titanite; Kamo and Davis, 1994). Although the granitoids south of the Pongola Supergroup have not been mapped and characterized in detail (largely because of poor outcrop) they have been dated previously at least three localities identified in the caption of Fig. 1B. The so-called “G4 Granite” gave an Rb–Sr whole-rock isochron age of 3163 ± 103 Ma (Allsopp, 1961); Natal Spa granite (part of the Anhalt – Speenkoppies suite; Fig. 1B) gave a single zircon U–Pb age of 3223 ± 2 Ma (Meyer et al., 1993); and the Anhalt leucotonalite, an Rb–Sr whole rock isochron age of 3250 ± 39 (Farrow et al., 1990). Recent precise ages of the Anhalt trondhjemite suite (at a locality known as the Eskay quarry) of 3222 ± 8 Ma and 3193 ± 5 Ma (Saha et al., 2010) are important as this granitoid is most likely basement to the Assegai supracrustal rocks which immediately predated the deposition of the Pongola Supergroup. Ages for the Ancient Gneiss Complex on the northeastern side of the Pongola Supergroup range from 3436 ± 6 Ma for the Tsawela Gneiss (Pb–Pb single zircon evaporation; Kröner and Tegtmeyer, 1994) to 3644 ± 4 Ma for the Ngwane Gneiss (U–Pb SHRIMP; Compston and Kröner, 1988).

A recent important advance in the understanding of the pre-Pongola basement rocks is the recognition of a previously poorly documented period of crustal growth at c.3.24–3.22 Ga (Schoene and Bowring, 2010) with a precise age determination for the Usutu suite of 3265.5 ± 0.5 (Locality of sample EKCO-64 in Fig. 6 of Schoene and Bowring (2010)). [Personal communication from Blair Schoene (2012) explains possible confusion arising from the locality of their sample being stated as coming from the Nhlangano gneiss suite (now agreed as referring to the post-Pongola granitoid), and suggests that in future it should be referred to by a different name consistent with the 3.26 Ga granitoid suite].

3.2. Post-Pongola granitoids

Although no dates were given, Hunter (1957) recognized on the basis of structural relations that the Hlatikulu granite and the Nhlangano gneiss were older than the Kwetta and Mswati Granites. Barton et al. (1983) dated the Hlatikulu granite and Nhlangano gneiss using the Rb–Sr method obtaining ages of 2417 ± 148 Ma and 2244 ± 355 Ma, respectively. The Hlatikulu granite was subsequently dated by Schoene and Bowring (2010) who obtained ages of 2728.9 ± 0.5 Ma and 2729.8 ± 0.4 Ma using chemical abrasion of zircons followed by isotope dilution – thermal ionization mass spectrometry. The Kwetta post-Pongola granite has yielded several contradictory dates: 2671 ± 3 Ma (single zircon, Meyer et al., 1993); 2520 ± 422 Ma (Rb–Sr whole rock isochron, Barton et al., 1983); and 2722 ± 6 Ma (Pb–Pb zircon evaporation, Maphalala and Kröner, 1993). Two post-Pongola samples from the Mswati Granite group have been dated: the Mooihook pluton at 2824 ± 6 Ma (Pb–Pb single zircon evaporation, Maphalala and Kröner, 1993) and the Mshlosheni pluton at 2286 ± 403 Ma (Rb–Sr whole rock isochron, Barton et al., 1983) and 2822 ± 5 Ma (Pb–Pb zircon evaporation, Maphalala and Kröner, 1993). The Rb–Sr whole rock data can largely be discounted as they do not lie within error of the later precise dating. However, the range of ages from precise methods spans over 100 million year. The ages presented by Schoene and Bowring (2010) are essentially in the middle of the range.

3.3. Ages for the Pongola Supergroup

A summary of ages obtained for the Pongola Supergroup is given in Table 1 with localities for sample sites of this study shown in Figs. 1A and 2. Burger and Coertze (1973) reported relatively old ages for the Nsuze Group of 3083 ± 150 Ma on rhyolite using the Rb–Sr method and 3090 ± 90 Ma using the zircon U–Pb method. These ages were from the southern area of the Nsuze Group and therefore do not lie within the area shown in Fig. 1B. More recent analyses of Nsuze rhyolites in the northern and central regions gave younger ages. Hegner et al. (1984) dated one sample (PO-84) using three different methods and obtained ages of 2940 ± 22 Ma (U–Pb zircon evaporation), 2934 ± 114 Ma (Sm–Nd whole rock isochron), and 2883 ± 69 Ma (Rb–Sr whole rock isochron). Later work by Hegner et al. (1994) re-analyzed the PO-84 sample using U–Pb on abraded zircons obtaining a slightly older but precise age of 2985 ± 1 Ma. The upper sedimentary Mozaan Group of the Pongola sequence has been dated at 2860 ± 26 Ma (whole rock Pb–Pb errorchron ages for ferruginous shale; Walraven and Pape, 1994).

Table 2
Summary of U–Pb ages.

Description	Sample #	Age	MSWD	Analysis used
Pre-Pongola				
Tsawela Gneiss (NE side)	CG-65	3427 ± 24	18	Regression[a]
Hoopwel area granite	CG-73	3267 ± 21	0.41	Regression[a]
Piet Retief area granite	PG-36	3147 ± 13	1.7	Regression[a]
Pongola				
Andesite (lowest unit)	CG-170	2980 ± 10	4.3	CalcAge[b]
		2980 ± 20	0.99	Pb/Pb Wtd Mean
Rhyolite (middle unit)	CG-171	2966 ± 10	0.49	Regression[a]
		2968 ± 6	0.00	CalcAge[b]
		2967 ± 9	0.61	Pb/Pb Wtd Mean
Andesite (highest unit)	CG-174	2954 ± 9	3.5	Pb/Pb Wtd Mean
Post-Pongola				
Nhlangano gneiss	CG-172	2963 ± 9	2.76	Pb/Pb Wtd Mean
Hlatikulu granite	PG-45	2973 ± 31	4	Regression[a]
	PG-44	2960 ± 11	0.62	Regression[a] Regression[a]
		2742 ± 22	1.3	
Kwetta Granite	CG-175	2911 ± 50	1.8	Regression[a]
		2721 ± 16		
	PG-49	2720 ± 10	0.81	Regression[a]
Mswati (Mhlosheni Pluton)	CG-173	2837 ± 6	2.4	CalcAge[b]
		2838 ± 10	0.48	Pb/Pb Wtd Mean
Mswati (Sicunusa Pluton)	CG-66	2717 ± 11	0.17	Regression[a]

[a] Regression ages calculated in ISOPLOT.
[b] CalcAge calculated as a bivariate weighted mean of $^{206}Pb^{*}/^{238}U$ and $^{207}Pb^{*}/^{235}U$ using ISOPLOT.

The U–Pb age of 2837 ± 5 Ma (Gutzmer et al., 1999) for an intrusive quartz porphyry sill cutting the Mozaan Group sediments provides a minimum age for the Mozaan Group. The Mooihoek granite (part of the Mswati granitoid suite, Fig. 1B) dated at 2824 ± 6 (Maphalala and Kröner, 1993) is undeformed and therefore these two ages constrain the period of folding of the Mozaan Group (Gutzmer et al., 1999). The entire age range from 3090 Ma to 2883 Ma, as represented by the Rb–Sr data, is unsatisfactory in assessing the tectonic setting and evolutionary history of the Pongola Supergroup and will not be included in further discussion. However, even for robust isotopic systems complexities may arise from inherited zircons in the highly silicic rocks, and will be discussed further.

The SHRIMP ages produced by Nhleko (2003) (Table 1) are a significant contribution to constraining the age of the volcanic rocks in general. Furthermore, the silicic character of the granitoids and some volcanic rocks make it highly likely that inherited zircon components are present in the suite and therefore multi-grain analyses conducted in some of the previous studies are likely to hide complexities that are more decipherable with spot analysis of individual grains by the ion microprobe technique.

Of importance in the genesis of the Pongola lavas is the age of the Usushwana Complex (Fig. 1B). Ages determined by Rb–Sr whole rock dated the complex at 2871 ± 30 Ma (Hegner et al., 1984), and 2875 ± 40 Ma (Layer et al., 1988) which would have precluded this complex as a staging chamber to the lower Nsuze volcanic series. The most recent and precise age determinations for the Usushwana Complex yielded ages of 2989.2 ± 0.8 Ma and 2989.8 ± 1.7 Ma (Olsson, 2012; presented with permission of the author) by isotope dilution – thermal ionization mass spectrometry for baddeleyite from gabbroic rocks from the eastern and western arms of the intrusion respectively (Fig. 1B; Table 1). On this basis the Usushwana Complex must be regarded as a possible early – stage magma chamber associated with the eruption of the mafic lavas of the Nsuze Group in this area.

4. Methods

4.1. Sample preparation

Samples were reduced in size using a jaw crusher and pulverized using a disc mill and high-density minerals were concentrated using the Gemeni water table, with further concentration carried out using bromoform and methylene iodide heavy liquids. Magnetic minerals and iron particles were removed using a hand magnet and the Frantz magnetic separator was used to further concentrate the zircons. The most pristine and optically clear zircon grains were selected for analysis using a binocular microscope.

These zircon grains were mounted in ∼2.5 cm-diameter epoxy discs with grains of zircon standards AS-3 (1099.1 ± 0.5 Ma; Paces and Miller, 1993) and 91,500 (1065.4 ± 0.3 Ma; Wiedenbeck et al., 1995). The mounts were polished approximately to the centers of the grains and back-scattered electron (BSE) and cathodoluminescence (CL) images were taken with the Hitachi S3200N scanning electron microscope and Cameca SX100 microprobe, respectively, at the University of Michigan to view the internal zoning, surface features, and inclusions where present. Carbon coating applied to the mounts before imaging was polished off, and the mounts were then cleaned in an ultrasonic bath of soapy water and rinsed in deionized water before being coated with gold for the ion microprobe analyses.

Whole rock sample powders for geochemical and isotopic studies were prepared from samples free of any visible surface weathering. Standard jaw crushing procedures were followed using a low-Molybdenum carbon steel crusher, and samples were powdered using a high-purity carbon steel shatter box. Samples were run in order from mafic to felsic (based on field identifications) to minimize cross-sample contamination.

4.2. SIMS analyses

Zircon grains were analyzed on the Cameca IMS 1270 high-resolution ion microprobe at the W.M. Keck Foundation Center for Isotope Geochemistry National Ion Microprobe Facility, University of California, Los Angeles (UCLA) using the standard operating procedures outlined in Harrison et al. (1995) and Quidelleur et al. (1997). Standards AS-3 and 91,500 were analyzed to obtain a curve of UO/U versus Pb/U relative sensitivity factor before running samples, and were then analyzed after every 4–5 unknowns throughout the data collecting process to track changes in instrument calibration. BSE and CL images were used to choose spots to analyze on grains in areas free of cracks and inclusions. The images also helped to identify possible inherited cores and metamorphic or igneous overgrowths, where present, so they could be dated separately. The ion microprobe primary beam was focused to a ~20 μm diameter ellipse for smaller grains (generally the volcanic samples) and for analyses of thinner zones that were considered important enough to evaluate. A larger, ~40 μm diameter spot size was used for larger grains, where possible, to obtain greater precision through higher count rates. Data were processed using the ZIPS program, and concordia diagrams were generated using the computer program ISOPLOT (Ludwig, 1999). Rregressions to obtain the concordia upper intercepts for discordant zircon populations were limited to spots exhibiting <20% discordance. This approach minimized the effects due to the evident multiple factors triggering discordance, such as metamorphism and metamictisation, which can cause Pb loss. When the points for a given sample were concordant and no regression was possible, the age was calculated using an error-weighted mean of the $^{207}Pb^{*}/^{206}Pb^{*}$ values.

4.3. Major and trace element compositions

The samples investigated for U–Pb isotopes and Nd isotopes were also analyzed for major and trace elements. Major elements were analyzed by X-ray fluorescence (Philips PW1404, University of Kwazulu-Natal) using fusion disks, following the method of Norrish and Hutton (1969). International reference materials BCR-1, AGV-1, NIM-N, DTS-1, GSP-1 and BHVO-1 were used as primary standards and then were compared to in-house standards, used as controls. Some trace elements were analyzed by X-ray fluorescence on pressed pellets by X-ray fluorescence using the NIM and USGS ranges of international reference materials. Rare-earth elements were analyzed using inductively coupled plasma mass spectrometry (ICP-MS) (Perkin Elmer 6100, University of Kwazulu-Natal). Primary calibration was against certified standard solutions, and the international reference materials BCR-1, BHVO-1 and RGM-1 were run as controls using the method of Wilson (2003).

4.4. Sm–Nd isotopic analyses

Standard dissolution and column procedures as described by Choi et al. (2008) were followed, after which each sample was dried to a solid, treated with a drop of 14N HNO_3, redried, and then loaded onto double rhenium filaments using a 1.5N HCl acid solution. The samples were then run on a Finnigan MAT262 thermal ionization mass spectrometer at the University of Michigan. Mass fractionations for the Nd ratios were normalized to $^{146}Nd/^{144}Nd = 0.721900$. Neodymium values obtained on the instrument for the La Jolla Nd Standard are $^{143}Nd/^{144}Nd = 0.511842 \pm 10$. Total Sm and Nd blanks averaged 0.02 ng. Sr isotopes were not measured given the inherent unreliability of these data from previous studies.

5. Results

5.1. U–Pb zircon ages

Samples of the pre-Pongola granitoids dated in this study were taken at Piet Retief, Hoopwell and Tsawela, with positions shown on Fig. 1B. The zircon grains for the three pre-Pongola granitoids dated in this study are all euhedral with magmatic oscillatory zones, and produced data with relatively small discordances. The analytical data and ages for all individual spot analyses are given in the supplementary data file entitled 'Zircon U/Pb data for spots analyzed by high-resolution secondary ionization mass spectrometry (SIMS)' A summary of ages for each sample is given in Table 2. Data for the pre-Pongola granitoids, shown graphically in Fig. 3a and b, give ages of 3147 ± 13 Ma for a sample from the Piet Retief area and 3267 ± 21 Ma for the Hoopwell area granitoid, to the east and

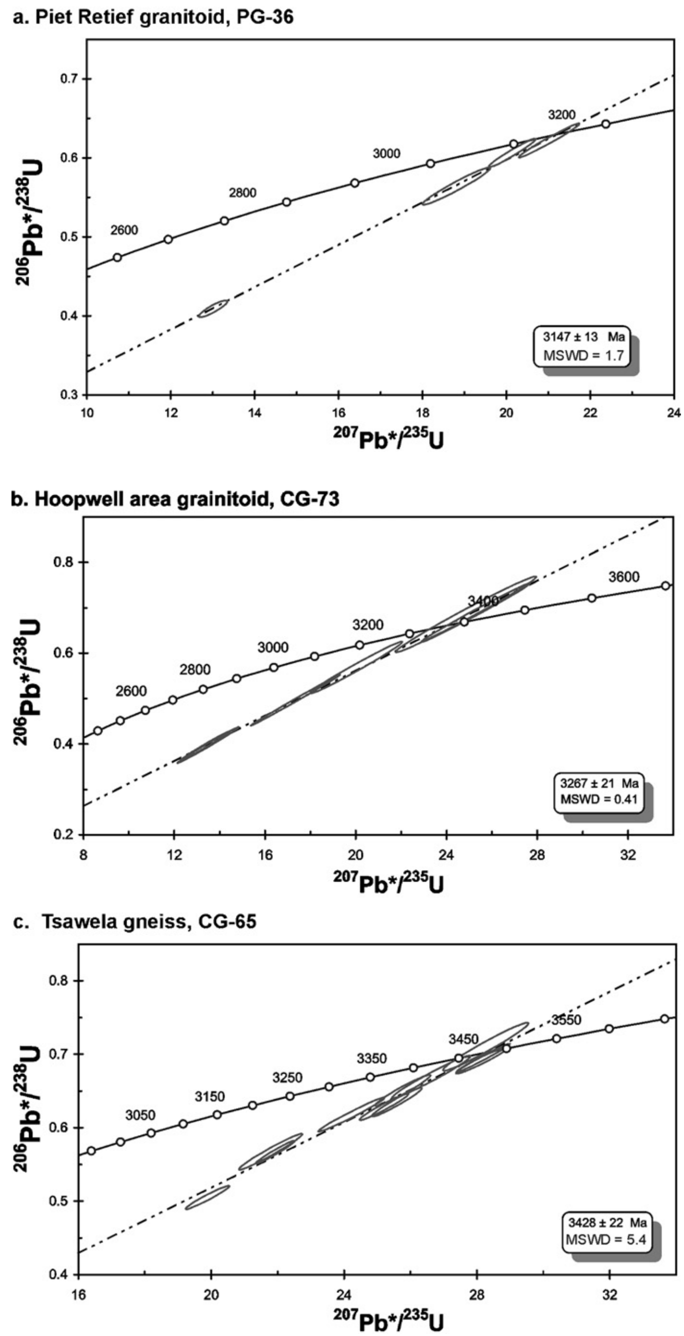

Fig. 3. Concordia plots for pre-Pongola granitoids. (a). Piet Retief area granitoid (PG-36): 3147 ± 13 Ma, (b). Hoopwel area granitoid (CG-73): 3267 ± 21 Ma, (c). Tsawela Gneiss of the Ancient Gneiss Complex (CG-65): 3427 ± 24 Ma. The age differences for the basement granitoids on the SW and NE sides of the Pongola Basin highlight possible different crustal blocks.

south of the town of Piet Retief (Fig. 1B). A sample (CG-65) from the Tsawela Gneiss (Fig. 3c) of the Ancient Gneiss Complex on the north side of the Pongola Supergroup depository gives an age of 3428 ± 22 Ma with an indication, based on point distributions, that there may be two zircon populations separated in age by just a few million years (Fig. 3c). These have not been assessed further.

As for the Pongola volcanic rocks, the small grain-size and limited number of zircons in some of these samples makes dating difficult. The sequence of Pongola volcanic rocks shows a progression in ages from the lowest exposed unit in the Nsuze Group (in the west) (Localities A and B on Fig. 2) to the highest volcanic flow present in the upper Mozaan Group (Point C on Fig. 1B). The

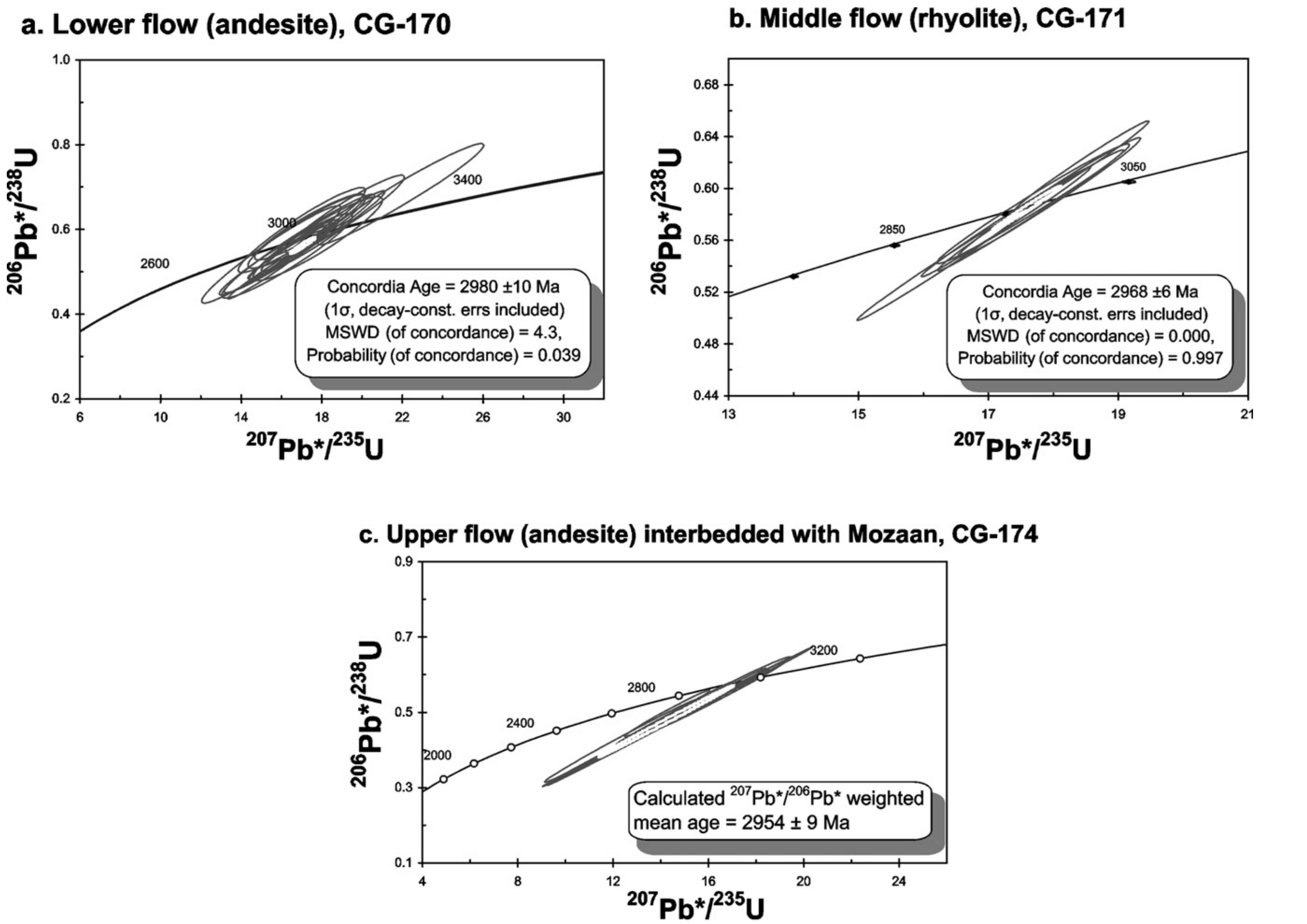

Fig. 4. Concordia plots for the Pongola volcanic rocks. (a) Lowest andesitic flow (CG-170): 2980 ± 10 Ma, (b) middle rhyolite flow (CG-171): 2968 ± 6 Ma, (c) upper andesitic flow interbedded with upper Mozaan Group (CG-174): points were slightly discordant, but give a Pb–Pb weighted mean age of 2954 ± 9 Ma.

sample from the stratigraphically lowest andesitic flow (CG-170) gives a concordia age (as defined by Ludwig, 1999) of 2980 ± 10 Ma (Fig. 4a). A middle-sequence rhyolite flow sample, CG-171, gives a concordia age of 2968 ± 6 Ma (Fig. 4b), and sample CG-174, taken from an andesite flow interbedded in the Mozaan, gives a $^{207}Pb^{*}/^{206}Pb^{*}$ weighted mean age of 2954 ± 9 Ma (Fig. 4c). The concordia plot for this sample (Fig. 4c) does not produce a meaningful regression age because of limited discordance unless it is assumed that the lower intercept age is 0 Ma. Therefore a Pb–Pb weighted mean age is calculated instead. A second flow from the middle of the Nsuze sequence gives a wide range of ages, with the youngest clustering at 2704 Ma and the oldest at >3400 Ma (diagrams and data not shown). The diverse populations make it impossible to get any chronologically meaningful information for this sample, but they hint at the complexity of mixing disparate components to produce some of the magmas from which theses rocks crystallized. The oldest zircons in this sample in the range ~3400–3600 Ma are similar in age to the Tsawela Gneiss and rocks in the Ancient Gneiss Complex, which suggests zircon inheritance in this Pongola andesite from the local basement rocks.

Ages yielded for the Nhlangano gneiss in Swaziland, immediately north of the South African border (Fig. 1B), are older than the Kwetta and Mswati Granites, and older than the age reported by Barton et al. (1983). The concordia plot for the Nhlangano gneiss (CG-172) (Fig. 5a), displays an upper intercept age of 2961 ± 14 Ma, and gives a $^{207}Pb^{*}/^{206}Pb^{*}$ weighted mean age of 2963 ± 9 Ma, which we consider to be the preferred age. This is older than the age of 2929 ± 5 Ma reported by Maphalala and Kröner (1993). Two additional samples, PG-45 and PG-44, were taken from the Hlatikulu granite and the zircon sample populations from both display distinctive cores and rims. The zircons from PG-45 have rose-colored, transparent cores with grey, cloudy metamict rims in transparent light. The BSE images show this same metamictisation of the rims (Fig. 6a), and consequently, high-precision analysis of the rims was impossible due to significant Pb loss. The concordia plot with five analyses from the non-metamict cores is shown in Fig. 5b and gives an age of 2973 ± 31 Ma. Zircons from sample PG-44 do not show any metamictisation, but include two distinct age populations that are easily distinguished from each other (Fig. 5c and d). The older age, 2960 ± 11 Ma is similar to that of sample PG-45, and the younger population of zircons gives an age of 2742 ± 22 Ma.

The sample from the Kwetta Granite (CG-175) also gives two ages (Fig. 7). A CL image of one representative zircon grain from sample CG-175 is shown in Fig. 6b. Distinct cores and rims, like those found in the Hlatikulu granite samples, are apparent. Two analyses from the core of this grain give an age of 2911 ± 50 Ma (Fig. 7a). The analyses from the rim give a younger upper intercept age of 2721 ± 16 Ma, similar to other grains analyzed in the sample (Fig. 7b). This younger age is consistent with previously published data for the Kwetta Granite of 2722 ± 6 (Maphalala and Kröner, 1993). Two other samples from the Kwetta Granite were analyzed. Sample PG-49 gives a well constrained concordia upper intercept age of 2720 ± 10 Ma (Fig. 7c). This is remarkably similar to the younger age obtained for sample CG-175.

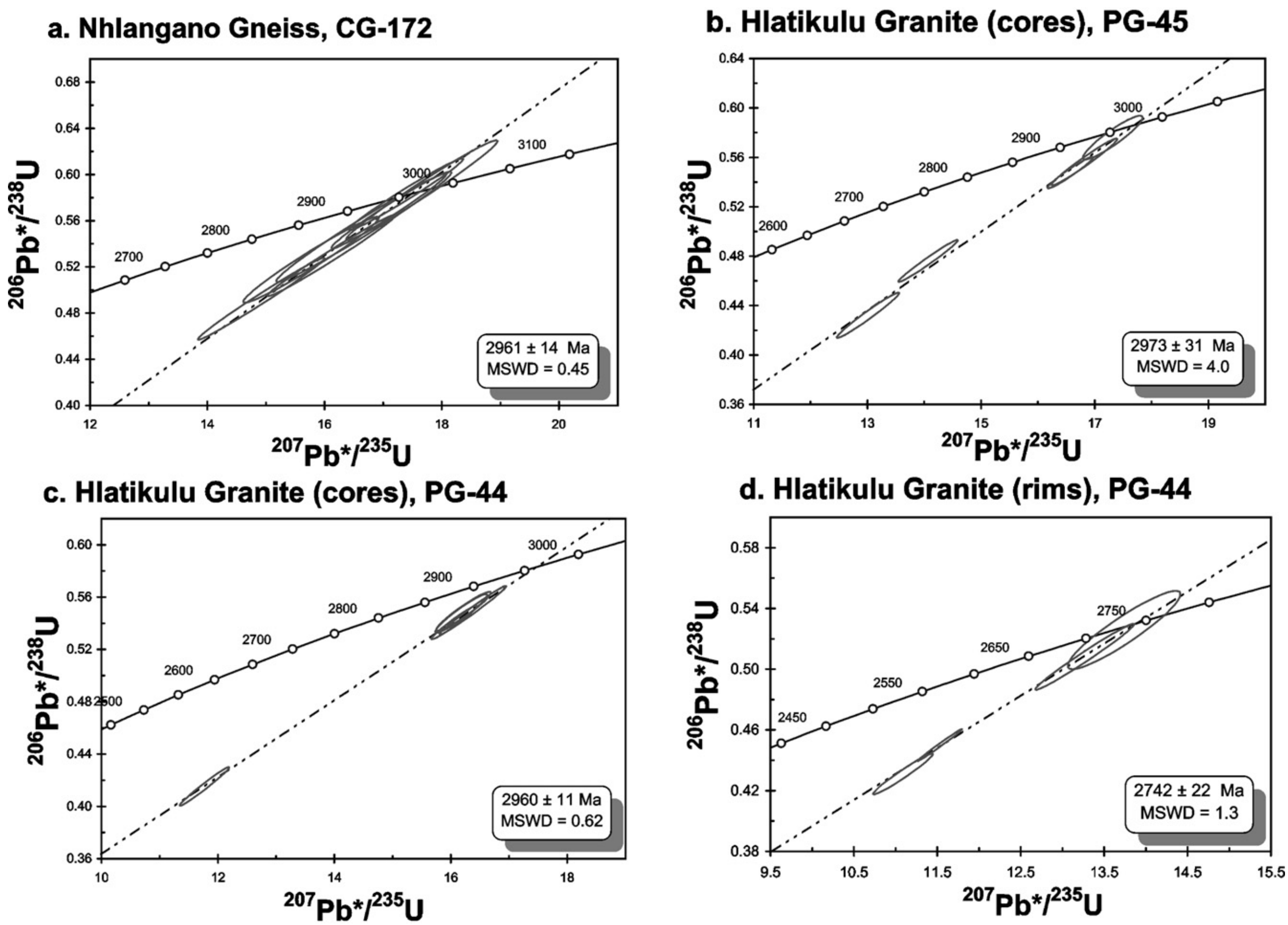

Fig. 5. Concordia plots for the older post-Pongola granitoids: (a) Nhlangano gneiss (CG-172): 2961 ± 14 Ma, (b) Hlatikulu granite (PG-45) cores: 2973 ± 31 Ma, (c) Hlatikulu granite (PG-44) cores: 2960 ± 11 Ma, (d) Hlatikulu granite (PG-44) rimes: 2742 ± 22 Ma.

The Mswati Granites were sampled at the Mhlosheni Pluton (CG-173: sample point M on Fig. 1B) and the Sicunusa Pluton (CG-66: sample point N on Fig. 1B). Analyses from these two samples (Fig. 8a and b) give ages of 2837 ± 6 Ma and 2717 ± 11 Ma, respectively. Although these ages are older than those reported by Barton et al. (1983), they are in agreement with the age of the Kwetta Granite, and are similar to the Pb evaporation isotopic ages reported by Maphalala and Kröner (1993) of 2723 ± 7 Ma for the Sicunusa Pluton and 2822 ± 5 Ma for the Mhlosheni Pluton.

5.2. Isotopic data

Results from the Sm–Nd isotope analyses of the Pongola volcanic rocks and post-Pongola granitoids are given in Table 3. $\varepsilon_{\mathrm{Nd}(t)}$ values get increasingly more negative from basalt to rhyolite ranging from −2.55 for CG-32 (basalt) to −4.20 for CG-9 (rhyolite). The post-Pongola granitoids also display negative $\varepsilon_{\mathrm{Nd}(t)}$ values ranging from −2.08 to −6.14. Calculated model ages for both the volcanic rocks and the granitoids are much older than the U–Pb ages for the same samples. T_{DM} values range from 3510 Ma to 3447 Ma for the volcanic rocks and from 3494 Ma to 3299 Ma for the granitoids.

Sm–Nd data shown graphically (Fig. 9) yield poor isochron ages of 3367 ± 410 Ma for the Pongola volcanic rocks and 2918 ± 170 Ma for the post-Pongola intrusives. $\varepsilon_{\mathrm{Nd}(t)}$ values calculated using the y-intercept are +0.2 for the Pongola volcanic rocks and −3.4 for the post-Pongola granitoids. The value for the Pongola volcanic rocks is not consistent with the universally negative values calculated for all of the samples. However, the value for the post-Pongola granitoids falls in the middle of the range calculated for the samples individually.

5.3. Geochemical data

5.3.1. Major elements

Major and trace element data for the Pongola volcanic rocks and the pre- and post-Pongola granitoids are given in the electronic supplementary data file entitled 'Major and Trace Element Compositions'. Data are given only for the samples used for geochronology and Nd isotopic studies, and therefore only generalized characteristics are discussed. An in-depth discussion of major and trace elements for the entire extent of the Pongola resulting from over 30 years of research is currently in preparation. Nevertheless, important characteristics are revealed in the present data set and it includes the first comprehensive geochemical data on the post-Pongola granitoids. Selected major and trace element data for the Pongola volcanic rocks, and the pre- and post-Pongola granitoids are shown in Fig. 10. The range in SiO_2 concentrations (50.5–74 wt.%), corresponds to MgO from 7 wt.% to 0.5 wt.% for the volcanic rocks (Fig. 10a), and covers the range from basalt to rhyolite with intermediate compositions also significant in volume. One of the volcanic rocks of intermediate composition (CG-174) is a basaltic andesite (based on SiO_2 content) with 5.7% MgO and 57.7% SiO_2 within the Mozaan Group, and is stratigraphically the highest sample of the volcanic suite. Both pre- and post-Pongola granitoid suites have less than 1 wt.% MgO. There is a wide range in $K_2O + Na_2O$ concentrations from 3.3 wt.% to 7.3 wt.% for the Pongola lavas (Fig. 10b). Both granitiod suites have relatively high contents of total alkalis and SiO_2. SiO_2 contents range from 69 wt.% to 78 wt.%. Al_2O_3 (Fig. 10c) shows a progressive decrease with increasing SiO_2 reflecting plagioclase fractionation, consistent with the plagioclase porphyritic character of the lavas of intermediate composition. The granitoids have relatively low Al_2O_3 contents with the post-Pongola suite having a range from 10.7 wt.% to 14.3 wt.% Al_2O_3. Iron content, expressed as Fe_2O_3 (Total Fe) in Fig. 10d, shows a wide range in the volcanic rocks from 14.5 wt.% to 4.6 wt.% in the rhyolite, but the trend is not coherent and this may reflect slightly different fractionation paths or Fe mobility during alteration. The granitoids contain less than 5 wt.% Fe_2O_3 (Total Fe). The trend for FeO (Total)/MgO (Fig. 10e) is one of higher ratios with increasing SiO_2 content in the volcanic rocks, and therefore reflects more rapid depletion of Mg compared to Fe in a fractionating system. The granitoids have low values for this ratio.

5.3.2. Trace elements

Trace element variation is shown in Fig. 10f–h for selected incompatible elements. Zr in the volcanic rocks shows a progressive increase with increasing SiO_2 (Fig. 10f), with the rhyolite showing extreme enrichment. One rhyolite has relatively depleted incompatible element contents, indicating possible differences in lineage for the fractionation paths. The pre-Pongola granitoids have low Zr contents and the post-Pongola granitoid suite has a wide range from 157 ppm to 665 ppm Zr. La rises systematically with increasing SiO_2 in the volcanic rocks (Fig. 10g). In the granitoids the pre-Pongola rocks have the lowest La contents whereas the post-Pongola granitoids are in the range of 57–186 ppm La. Th is lowest in the basalt (0.4 ppm) with the intermediate rocks containing 5–10 ppm, and rising to 30 ppm in the rhyolite (Fig. 10h). The pre-Pongola granitoid suite is depleted in Th, but the post-Pongola suite is strongly enriched in Th, with the highest value reaching 74.8 ppm.

The REE data normalized to primitive mantle using values of McDonough and Sun (1995) (Fig. 11) for the lavas have relatively steep negative slopes for the LREE and flat patterns for the HREE. Overall, concentrations for all REE increase with decreasing MgO content in the volcanic rocks. The basalt has a relatively flat REE pattern with a small positive Eu/Eu* anomaly. The more evolved rock types have a progressively more pronounced negative Eu/Eu* anomaly. The andesite (CG-174) has a negative Eu/Eu* anomaly and also has a crossing REE pattern. This sample (CG-174) is from the Tobolsk Formation in the Mozaan Group and may indicate a different magma source compared with the other volcanic samples. The rhyolites have steep LREE patterns and relatively flat HREE consistent with their derivation from pre-existing crustal protoliths. The felsic lavas have pronounced negative Eu/Eu* anomalies (0.52 for PG-171) indicating plagioclase fractionation. The pre-Pongola samples have quite steep patterns for the LREE, and the HREE range from flat to steep with a turn-up from Er to Lu for one sample, suggestive of melting of garnet in the source of these rocks in evolved crustal rocks. The post-Pongola granitoids have steep LREE patterns and steep to relatively flat HREE patterns and extend over a wide range of REE concentrations. The highest REE concentrations in this suite are approximately twice that of the rhyolite. The striking feature of the post-Pongola granitoids is the marked Eu/Eu* anomaly (0.22–0.51). For some samples of the post-Pongola granitoid suite, there is a close overlap with the Pongola rhyolites, possibly reflecting a common source, and perhaps even derivation of the post-Pongola granites by melting of the Pongola volcanic rocks at depth.

Trace element distribution diagrams normalized to primitive mantle (McDonough and Sun, 1995) and arranged in order of increasing incompatibility (Fig. 12) illustrate both similarities and differences for the different suites. Significant negative anomalies are observed for Nb, Ta, P and Ti. In detail the Nb and Ta

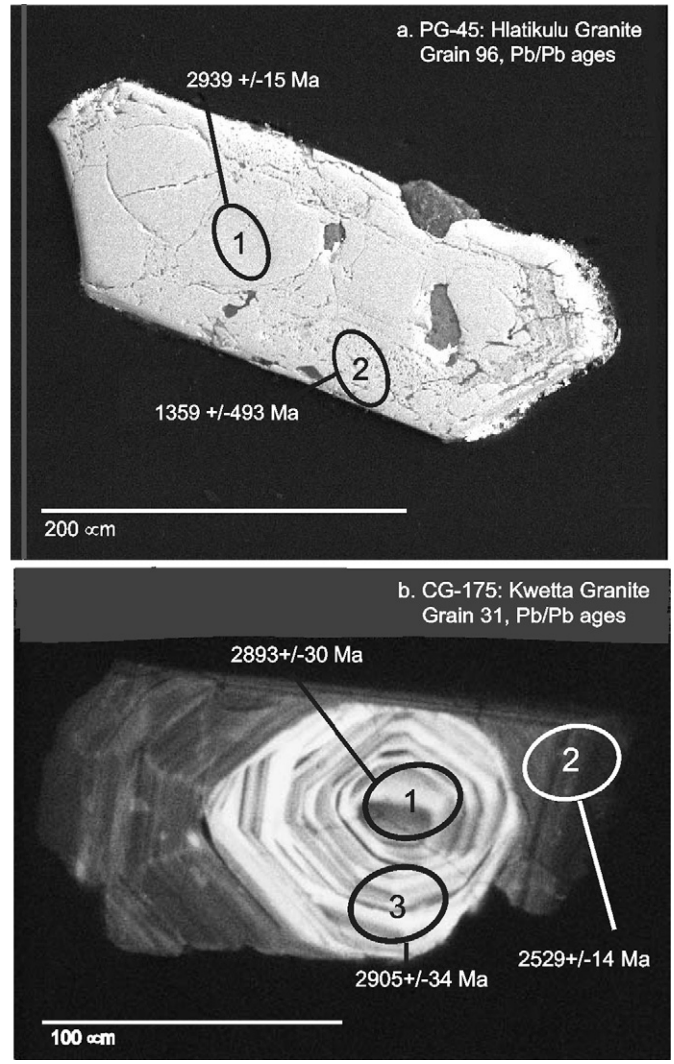

Fig. 6. Images of zircons from two samples taken from the Hlatikulu and Kwetta Granites showing distinctive cores and rims. (a) Back-scattered electron (BSE) image of a typical zircon from sample PG-45: *Hlatikulu granite*. The rims of sample PG-45 show extensive metamictisation making it impossible to obtain a date for this portion of the grain. Cores give a regression age of 2973 ± 31 Ma (see Fig. 5b). (b) Cathodoluminescence (CL) image of a representative zircon from sample PG-175: *Kwetta Granite*. Two spots from the core of this grain were analyzed giving a regression age of 2911 ± 50 Ma. Data for this rim are consistent with data from other grains from this sample giving an age of 2721 ± 16 Ma (see diagrams in Fig. 7). Note: Ages on diagrams are based on individual points and are not the same as regression ages.

anomalies relative to Th are less pronounced for the primitive basalts, but become increasingly so for the intermediate rocks and the rhyolites. The basalts and basaltic andesites have low values for La/Th (average 0.11), typical of oceanic basalts (Plank, 2005), whereas this ratio for felsic rocks is 0.23, and 0.5 for the post-Pongola granitoids indicting a progressive amount of subducted material included into the felsic component, rather than fractionation of a basaltic parent as suggested by Armstrong et al. (1986).

6. Discussion

6.1. Interpretation of ages

The ages of the pre-Pongola granitoids are interpreted to represent the time of emplacement and are consistent with those reported previously in the literature. The Tsawela Gneiss of the Ancient Gneiss Complex on the northeastern side of the Pongola

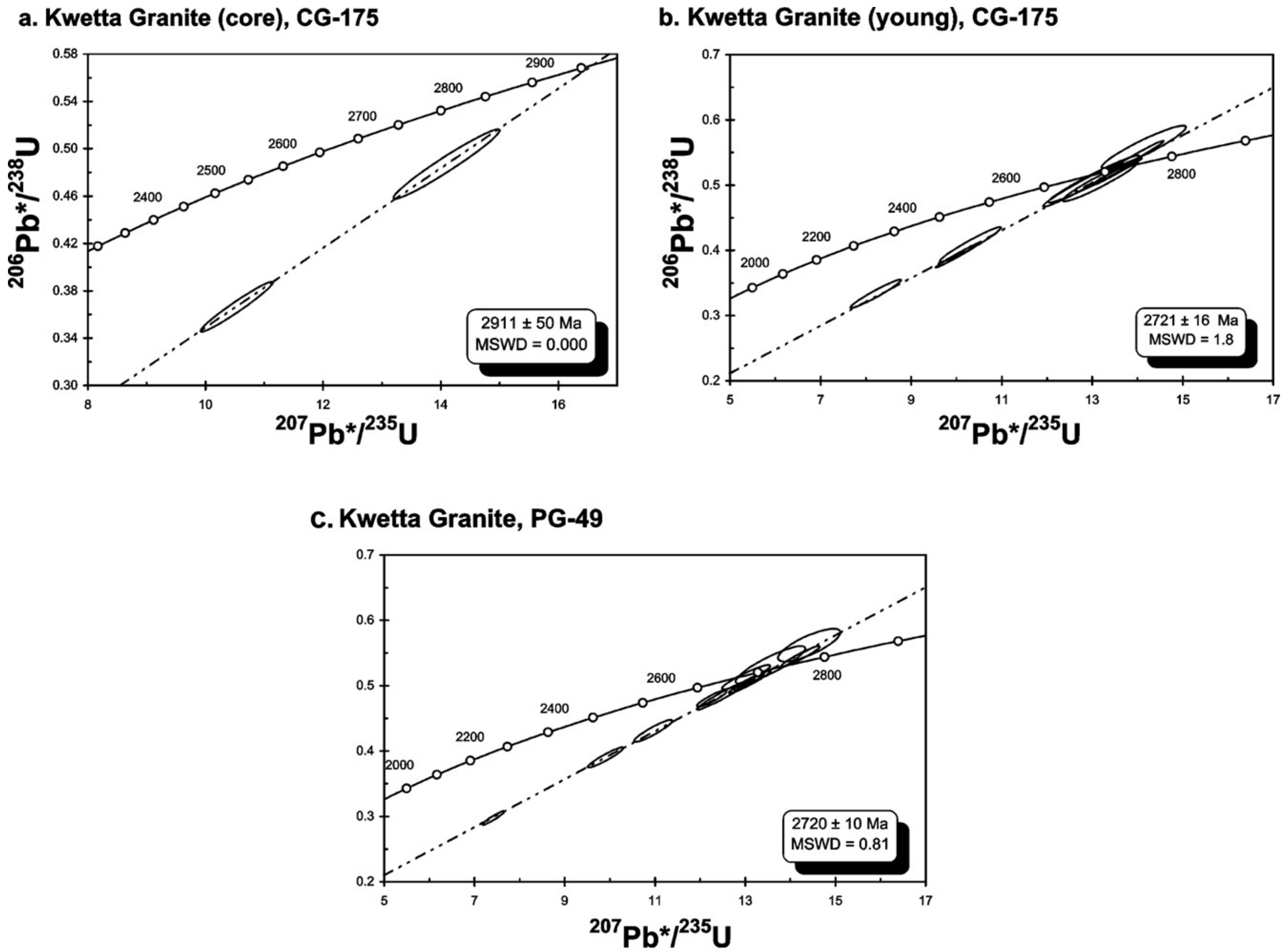

Fig. 7. Concordia plots for the younger post-Pongola Kwetta Granite: (a). CG-175, core of grain 30: 2911 ± 50 Ma, (b) CG-175, younger age: 2721 ± 16 Ma, (c) PG-46: 3103 ± 19 Ma, (d) PG-49: 2720 ± 10 Ma.

depository is 3427 ± 24 Ma, consistent with the Pb–Pb single zircon evaporation age of 3436 ± 6 Ma reported by Kröner and Tegtmeyer (1994). This rock unit is significantly older than that for any of the granitoids measured on the southwestern side of the Pongola depository, which yielded ages of 3147 ± 13 Ma and 3267 ± 24 Ma and which agree with age determinations from previous studies (Allsopp, 1961; Farrow et al., 1990; Saha et al., 2010). These granitoids are therefore older than the 3107 + 4/−2 Ma Mpuluzi sheet granite northeast of the central Pongola outcrop area, which was dated by Kamo and Davis (1994).

We have reported three reliable dates for the Pongola Supergroup: one from the stratigraphically lowest andesitic section (CG-170), one from a middle rhyolitic section (CG-171), and one from an andesitic section interbedded with the upper Mozaan Group (CG-174) (Figs. 1 and 2). These samples constrain the time of emplacement for the Pongola Supergroup in the northern area to between 2980 ± 10 Ma and 2954 ± 9 Ma, which, by taking into consideration the determined analytical errors, represents a time span for the combined depositional event of both the Nsuze and Mozaan successions to between 7 and 45 million years. The relatively old age obtained for the Tobolsk andesite (CG-174) is at variance with current estimates of the age of Mozaan Group but is the first direct age determination of this unit. The age of 2837 ± 4.7 Ma by Gutzmer et al. (1999) is a minimum age and therefore the Mozaan may be considerably older than this. The only other age determination for the Mozaan Group was by Walraven and Pape (1994), a Pb–Pb age of 2860 ± 26 Ma for a ferruginous chert. The ages on detrital zircons from Nhleko (2003) show a clear population peak at 2950 Ma corresponding to the age obtained in this work for the Tobolsk andesite. Rare zircons from Nhleko (2003) give younger ages from 2944 Ma to 2902 Ma. These detrital zircons are from sediments that occur stratigraphically lower in the succession than the Tobolsk andesite. Therefore, while inheritance of older zircons yielding the older age presented here must be considered a possibility, the zircons may have been derived from other volcanic layers that have since been eroded but deposited over a narrow time interval for the whole succession. Considering the errors from our age determinations, the maximum depositional time span for the whole sequence is 45 million years and that for the Mozaan Group is 29 million years. As a working scenario, and using the ages determined in this study and adopting the stratigraphic thickness of 8600 m as estimated by Gold (2006) for the central Hartland area, this translates into an accumulation rate of 0.19–1.2 mm/yr, which is within the range reported for modern environments with arc volcanism and interlayered sediments (e.g., Hildreth and Lanphere, 1994; Gamble et al., 2003; Bacon and Lanphere, 2006; Jicha and Singer, 2006; Singer et al., 2008). On the basis of these ages, and assuming the top of the Nsuze Group, the maximum rate of deposition of the Mozaan Group up to the level of the Tobolsk Formation (4000 m) would have been 0.14 mm/yr.

The Nhlangano gneiss gives the oldest age among the post-Pongola granitoids at 2961 ± 14 Ma and is consistent with its gneissic character as being the oldest of the post-Pongola granitoid

Table 3
Sm–Nd isotopic data.

Sample	Sm (ppm)	Nd (ppm)	$^{147}Sm/^{144}Nd$	$^{143}Nd/^{144}Nd$ ($\pm 2\sigma$)	U–Pb age (Ma)	$^{143}Nd/^{144}Nd$ (initial)	ε_{Nd} ($\pm 2\sigma$)	T_{DM} (Ma)	T_{CHUR} (Ma)
Basalts									
CG-32	2.056	8.792	0.1413185	0.511424 (14)	2970	0.508187	−2.55	3462	3310
CG-22	2.715	12.120	0.1354001	0.511266 (10)	2970	0.508122	−3.37	3510	3380
Andesites									
PG-24	9.848	46.195	0.1288378	0.511136 (11)	2970	0.508179	−3.40	3469	3345
PG-26	6.213	31.287	0.1200040	0.510941 (12)	2970	0.508200	−3.82	3453	3342
Rhyolites									
CG-9	6.891	36.879	0.1129195	0.510783 (11)	2970	0.508208	−4.20	3447	3345
CG-171	13.567	n.d.	n.d.	0.511057 (11)	2970	n.d.	n.d.	n.d.	n.d.
Post-Pongola granitoids									
PG-44	11.888	65.568	0.1095659	0.510800 (11)	2960 (2742)[a]	0.508407	−2.69 (−4.89)[a]	3303	3188
PG-45	12.137	54.542	0.1344900	0.511256 (14)	2978	0.508154	−3.19	3487	3355
PG-46	6.328	27.939	0.1368873	0.511308 (10)	2978	0.508144	−2.08	3494	3358
PG-49	18.113	110.486	0.0991000	0.510575 (10)	2720	0.508414	−6.14	3299	3195
CG-173	11.184	49.239	0.1372701	0.511330 (10)	2968	0.508184	−2.85	3465	3324

[a] The crystallization age is given for the core and the rim (in brackets) of the zircon grain. The $\varepsilon_{Nd(t)}$ is also given for the core and the rim, respectively.

and contemporaneous with the waning stages of Pongola volcanism. This is at variance with the age of c.3260 Ma age quoted for the 'Nhlangano gneiss' by Schoene and Bowring (2010). This problematic difference arises from interpretation of unit names and stems from the fact that the samples they analyzed came from the body to the north of the type intrusion in the vicinity of Nhlangano town, whereas the age of the Nhlangano gneiss, obtained in this study, is from the domed intrusion close to the town in the southwest (sample position G in Fig. 1B). As noted earlier in the personal communication from Blair Schoene, he recommends that a new name should be considered for the 3260 Ma rock unit to avoid confusion in the future. Zircon grains from our sample of the Nhlangano gneiss did not have distinct cores and rims potentially developed at different times, and therefore the obtained date is taken to be the time of crystallization for the rock.

Spots analyzed within the cores of both the Hlatikulu and Kwetta Granites give similarly older ages. The rims of these samples (where not highly metamict) give younger ages of 2742 ± 22 Ma and 2721 ± 16 Ma. Older ages are interpreted to represent

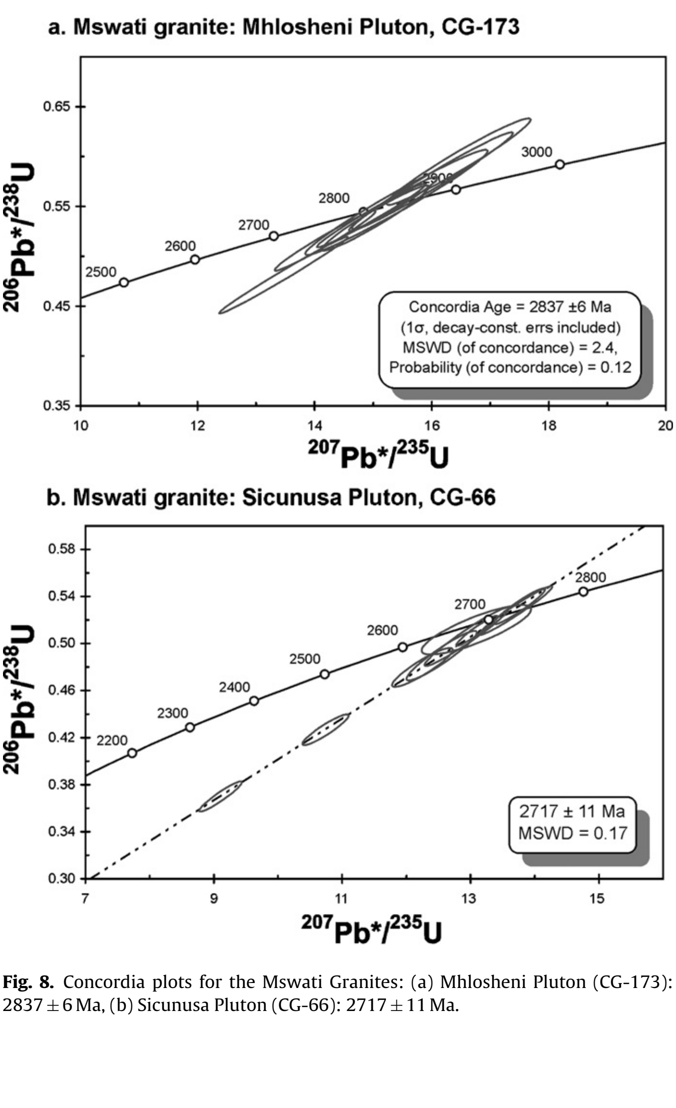

Fig. 8. Concordia plots for the Mswati Granites: (a) Mhlosheni Pluton (CG-173): 2837 ± 6 Ma, (b) Sicunusa Pluton (CG-66): 2717 ± 11 Ma.

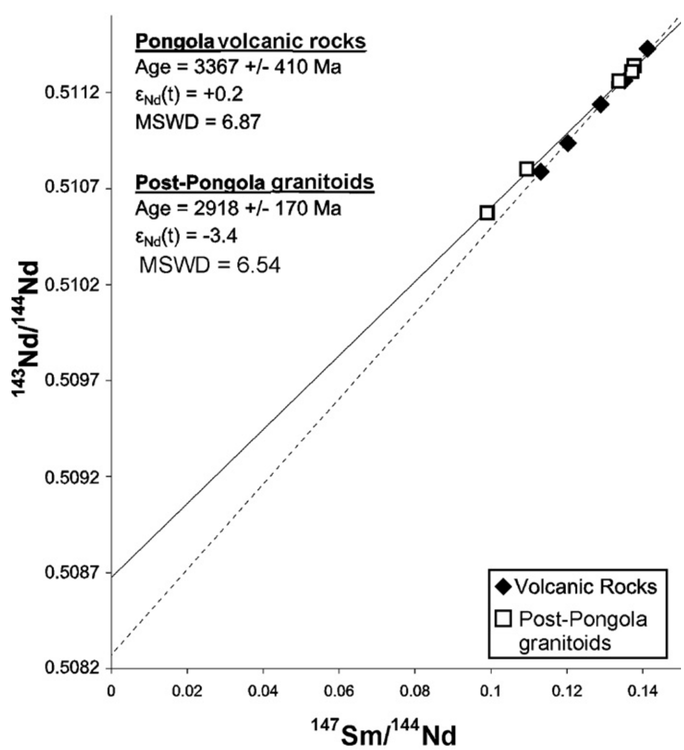

Fig. 9. Sm–Nd isochrons for the Pongola volcanic suite and the post-Pongola granitoids: the solid line is based on five samples from the Pongola volcanic suite; the dashed line is for five samples from the post-Pongola granitoid suite. The data are shown in Table 3.

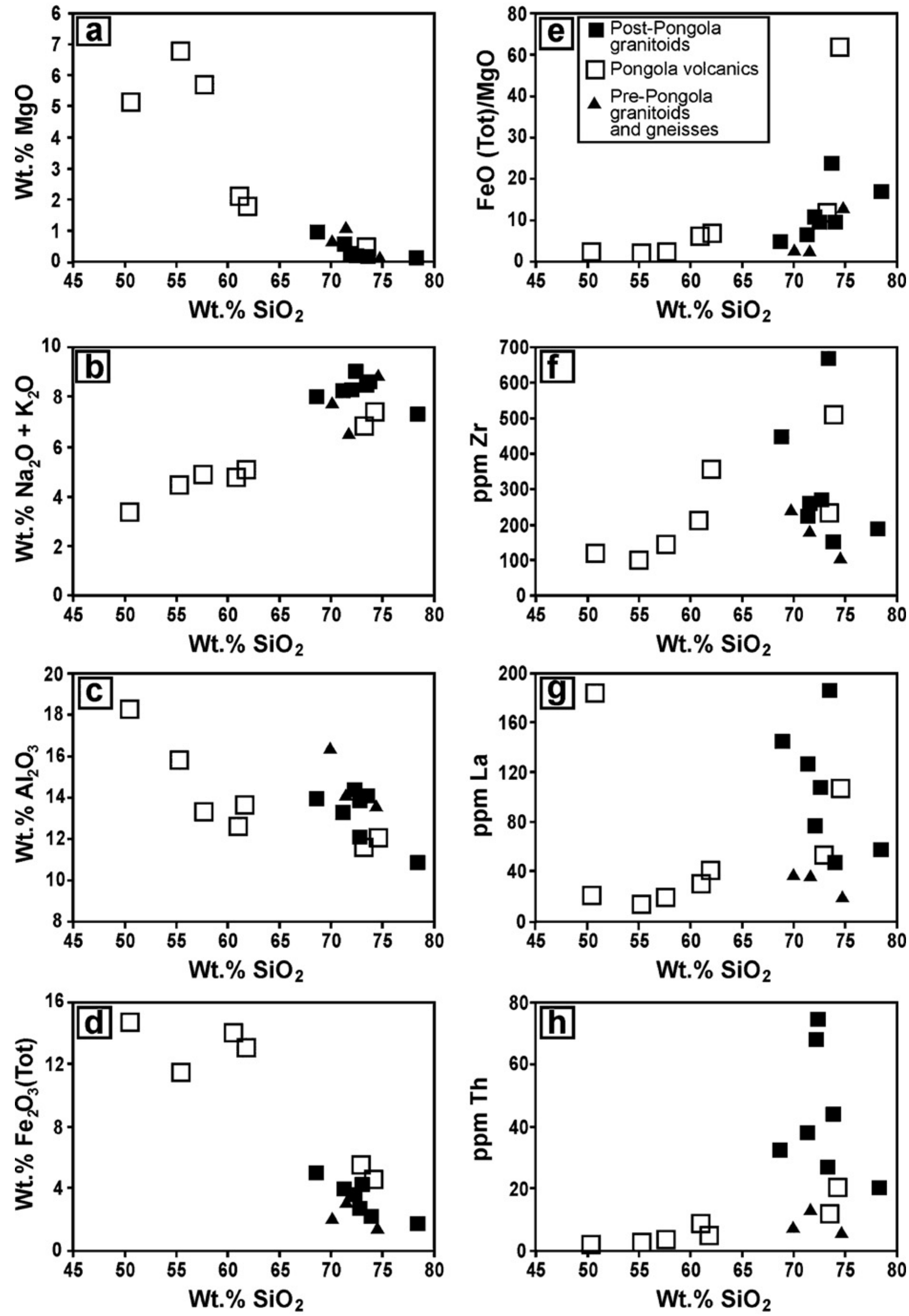

Fig. 10. Selected major oxide and trace element variation diagrams plotted against SiO_2. For the Pongola lavas the range of compositions from basalt to rhyolite is demonstrated. The compositions of the granitiod suites overlap for the major elements but are clearly distinguished by the incompatible elements La and Th with the pre-Pongola granitoids depleted in these elements whereas the post-Pongola granitoids are significantly enriched.

inheritance and the younger ones are considered to represent time of crystallization. This age is consistent with the previously published Pb–Pb zircon evaporation age for the Kwetta pluton (Maphalala and Kröner, 1993). The Nd model age for the Kwetta pluton is 3299 Ma, which is more than 500 million years older than the zircon U–Pb ages. It is possible that this age difference represents the crustal residence time of the materials reprocessed during the subsequent episode of melting. It also implies that these Archean granitoids were formed by multiple episodes of melting of diverse protolithic materials. Both CG-175 and PG-46 from the Kwetta Granite give old ages of 2911 ± 50 Ma and 3103 ± 19 Ma respectively, though each age is based on only two points, as all others show extreme Pb loss. It is deduced that the zircons in these plutons were inherited during magma generation from the pre-Pongola basement granitoids. The inheritance of these cores from rocks so close in age to the time of pluton crystallization suggests that crustal recycling was occurring during the mid-Archean on a time scale as short as 200 myr. Except for the very coarse-grained sample (PG-49), similarity in ε_{Nd} values for the post-Pongola granitoids (−2.08 to −3.19) and Pongola volcanic rocks (−2.55 to −4.20) indicates that either they had the same parental source or they experienced similar crustal contamination during ascent.

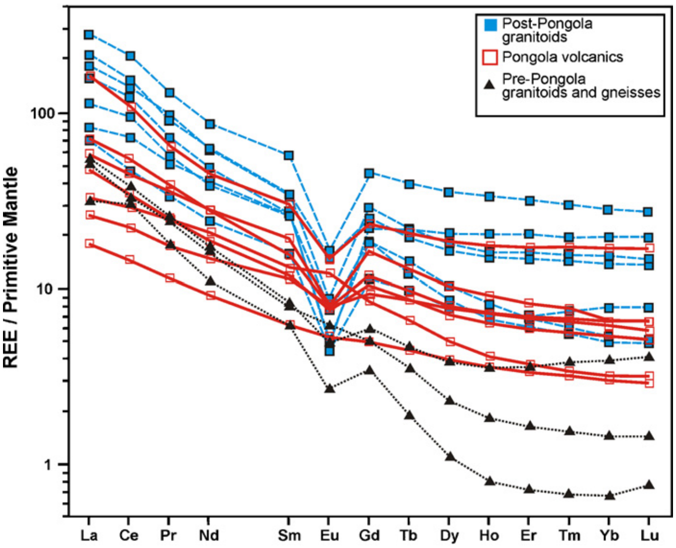

Fig. 11. Mantle-normalized rare-earth patterns for the Pongola volcanic rocks and the pre- and post-Pongola granitoids. The lavas show increasingly steep patterns and greater development of the Eu anomaly in the more evolved types. The pre-Pongola granitoids have steep REE patterns and flat HREE patterns whereas the post-Pongola granitoids have the greatest enrichment in REE and have deep negative Eu anomalies.

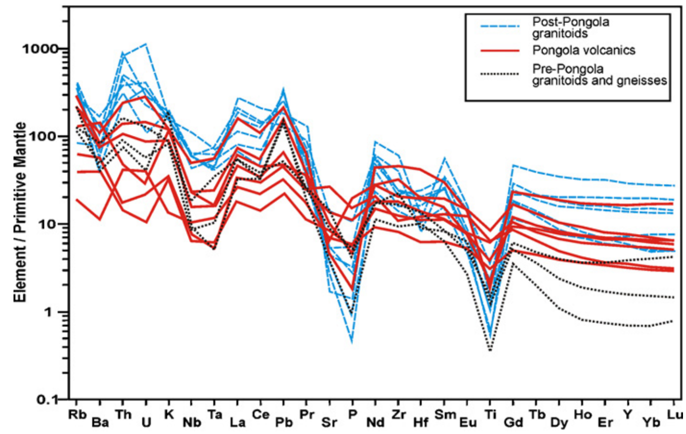

Fig. 12. Mantle-normalized trace elements (after McDonough and Sun, 1995) arranged in order of increasing incompatibility for the Pongola volcanic rocks and the pre- and post-Pongola granitoids. The patterns are similar for the rhyolite and some of the post-Pongola granitoids indicating a common source. The pre-Pongola granitoids are strongly depleted in the highly incompatible elements and less so for elements such as U and Th.

The strongly negative $\varepsilon_{Nd(t)}$ values ranging from −2.08 to −6.14, confirm that the protoliths were enriched materials in the crust and/or lithospheric mantle. The small spread in the Sm–Nd isochron data caused the large error. In addition, U–Pb data show a large spread in ages suggesting that these rocks were not cogenetic and therefore cannot be plotted together to produce a meaningful Sm–Nd isochron.

6.2. Significance of the geochemical signatures

The variations and scatter shown in the major element plots (Fig. 10) for the Pongola volcanic units are similar to those of the Armstrong et al. (1986) data set. Possible causes of the scatter include flow inhomogeneity, inherent magma characteristics derived from variable source components, variable early-stage contamination, and element mobility due to later alteration processes, and also domainal considerations in the complex interactions of volcanoes and flow sheets preserved in this area. Also similar to the results reported by Armstrong et al. (1986) are the REE and primitive mantle-normalized element discrimination diagrams for the Pongola lavas, with similar troughs in Eu, Ba, Nb, Sr, P and Ti. In addition, this study shows a negative anomaly in Ta that was not previously documented. The patterns show increasing overall enrichment with increasing SiO_2 concentration, but decreasing enrichment for Eu, Sr and P. This is consistent with advancing fractional crystallization and retention of these elements in mineral phases such as plagioclase and finally, apatite. High Sr/Y values of the majority of the pre-Pongola granitoids are probably due to Sr enrichment in Ca-plagioclase during magma differentiation. The low Sr/Y values exhibited by the Pongola lavas are likely to be due to plagioclase fractionation.

Ratios of Th/Yb versus Nb/Yb reveal source components and mobility of Th during melting of a subducting slab (Pearce, 2008; Bédard et al., 2012). Melting of the subducting slab adds Th to the source but does not change the ratio of Nb to Yb. Therefore contributions of an arc component would result in an array parallel to the OIB–MORB array. Bédard et al. (2012) point out that Archean magmas that are not subduction derived show oblique arrays that are not parallel to the OIB–MORB trend and reflect contamination by a crustal component. The Pongola lavas and the granitoids form an array parallel to the OIB–MORB trend, but also pass through the composition of continental crust (Fig. 13) which is dissimilar to the lava compositions of many greenstone belts and could suggest an arc environment. Therefore, while crustal contamination is clearly an important component of the Pongola rocks they may equally have inherited signatures relating to subduction processes.

The origin and tectonic setting of the post-Pongola granitoids remains a largely unresolved issue, but the present data contribute to the framework of understanding the operative processes. While the tectonic setting of the Nsuze Group remains uncertain, the post-Pongola granitoids are undeformed, have primary igneous fabrics, and were emplaced following the Pongola Supergroup when the craton had completely stabilized. They would then meet structural criteria for A- (anorogenic) type granites as defined by Loiselle and Wones (1979). They also meet the chemical criteria of Eby (1990) by having relatively low CaO and Al_2O_3, high $Na_2O + K_2O$ and K_2O/Na_2O and high $Fe_2O_{3(Total)}/MgO$. Incompatible trace elements (Zr, Nb, Y and Ta) are relatively high whereas lithophile elements (Sc, Cr, Co, Ni and Sr) have low abundances. Abundances of both HREE and LREE are high, but with a deep negative Eu anomaly (Fig. 11). Other discriminatory diagrams (Eby, 1990) which support the A-type granite are the relatively high

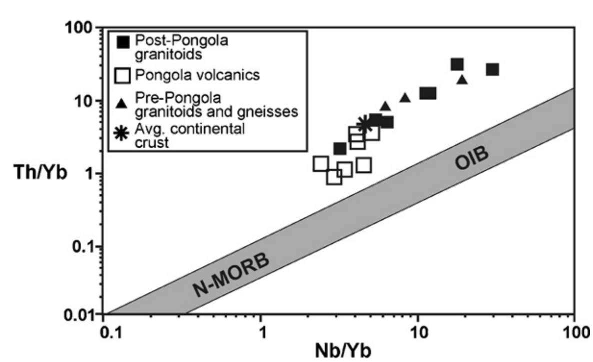

Fig. 13. Th/Yb versus Nb/Yb for the Pongola volcanic rocks and the pre- and post-Pongola granitoids using the diagram from Pearce (2008). Parallelism to the N-MORB/OIB array could imply metasomatic enrichment of Th in the source as could occur in a subduction melting. Simple contamination by crustal material of a primitive source would result in an oblique array. The array of the granitoids and the rhyolites passes through the composition of average continental crust whereas the basalts and basaltic andesites form a slightly displaced parallel array.

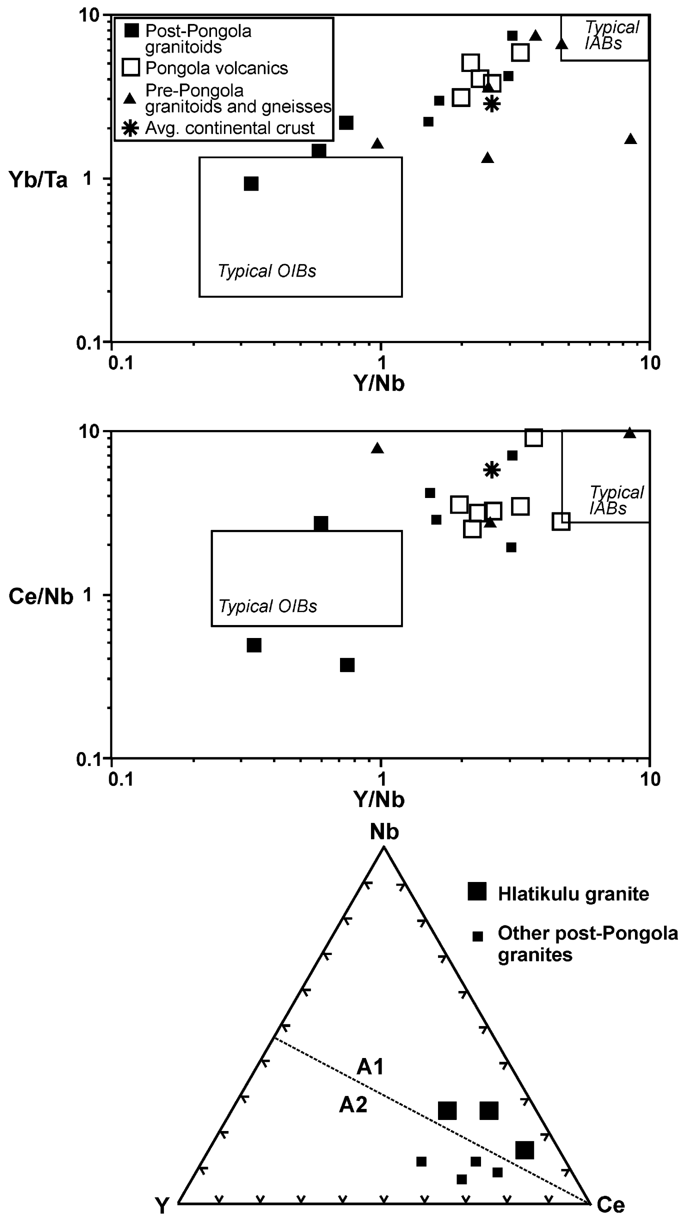

Fig. 14. Yb/Ta versus Y/Nb, and Ce/Nb versus Y/Nb diagrams after Eby (1990) demonstrate coherency in the A-type granitiod suite with the Pongola lavas. The pre-Pongola granites are also plotted. The lavas show restricted distribution as might be expected from fractionation control while the A-type post-Pongola granitoids are widely spread indicating the different bodies were derived from subtly different sources. The Hlatikulu granite is enriched in Nb compared to other post-Pongola granitoids.

ratios of selected incompatible elements (averages for Yb/Ta = 3.08; Y/Nb = 1.8; Ce/Nb = 4.84). The petrogenesis of A-type granite may involve several protoliths, but possibly the most applicable in this case is the derivation from previously melted crust (Collins et al., 1982). The relatively high values for Yb/Ta and Y/Nb (Fig. 14) are consistent with generation in post-collisional or post-orogenic and anorogenic environments (Eby, 1992). The post-Pongola A-type granitoids were most likely generated by second-order processes involving melting of crust. The A-type granites lie close to the boundary of the A1 and A2 sub-types defined by Eby (1992) on the basis of incompatible trace element ratios. One of the rhyolites (CG-171) is highly enriched in incompatible elements and has similar values for the discriminatory elements and ratios used to identify the post-Pongola A-type granites. This suggests that the granites may have been derived by melting of the Pongola rocks at depth. The major- and trace element compositions of sample CG-171 closely approximate the mean value of 11 rhyolite samples studied by Armstrong et al. (1986).

6.3. Tectonic setting

The Nsuze Group of the Pongola Supergroup spans the entire range of basalt–andesite–dacite–rhyolite compositions, but based on existing data is probably dominantly bimodal in compositional distribution with the main rock types being basaltic andesite and rhyolite. Basalt is a relatively minor component, which is markedly different compared to most Archean greenstone belts. Smaller amounts of intermediate rock type (andesites and dacites) may be attributed to variable contamination of basaltic magmas which is consistent with $\varepsilon_{\mathrm{Nd}(t)}$ becoming increasingly negative for the more siliceous lava types. There is currently insufficient field data in this study (or previous studies) to quantitatively assess the true relative volumes of the different rock types.

Convergent margins can juxtapose rocks of different origins, ages and with different chemical and isotopic signatures, thereby complicating our ability to deduce the original geodynamic settings. In contrast, it is expected that the rock units from either side of a rift can be traced across contrasting terranes if the original geometry is still discernible. The 3.6–3.4 Ga Ancient Gneiss Complex is present only on the northeastern side of the depository whereas the c.3.2–3.1 Ga terrane denominates the southwestern areas (with remnants of older greenstone belts), but gneissic rocks of this age also occur on northeastern side. This study is in accord with previous investigations and indicates that the preservation of the Pongola Supergroup may be attributed to a zone of weakness between contrasting crustal blocks, but this is not to suggest that the Pongola rocks unequivocally represent a subduction setting.

The basalts and basaltic andesites are the most primitive of the volcanic rocks, and their REE and high field strength element patterns are largely a reflection of source material composition and the melting process. Basalts, basaltic andesites and andesites in arc settings rarely exhibit Eu anomalies (McLennan and Taylor, 1981) and though some of the basalts and basaltic andesites of the Nsuze Group show slight positive or negative Eu anomalies, the overall REE trend and patterns on element distribution diagrams most strongly resemble those of modern arcs, and less so those of continental rifts.

Primitive mantle (PM)-normalized distribution plots of modern active continental margins, such as the Andes, have high enrichments in incompatible elements except for notable negative troughs in Nb and Pr and positive spikes in U and Pb. These patterns are similar to the basalts and basaltic andesites in the Nsuze Supergroup, including a Ta negative anomaly, and might be indicative of a convergent tectonic setting. However, these are features shared with continental crust, and therefore could have been inherited by interaction of primitive magmas with such material.

While the tectonic setting is not clearly identifiable there are both chemical and field indicators that constrain or eliminate some settings. Several controls may also superimpose similar signatures. A continental rift setting for the Nsuze lavas is least supported by field observations and the geochemistry, and the range and nature of the volcanic rocks. Similarly, the bimodal distribution and the high proportion of basaltic andesite and andesite are not consistent with supracrustal continental eruptions. The amount of volcaniclastic component in the Nsuze of the central region is also probably underestimated because of the apparently massive nature of the rocks, but recent detailed studies have shown much of this material to be fine-grained bedded ash deposits. Crustal contamination may impose characteristic signatures, such as depletion of Ta and Nb, but this would also be consistent with an active continental margin with the largely subaerial depositary supported by thick continental crust. Other plate tectonic models should also be considered, although these are unlikely to have been identical to recent and modern analogues. Extensional continental arc basins with rapidly deposited volcanic and sedimentary sequences (Busby, 2012, 2004; Barnes et al., 2001) are important crust building processes and may also have occurred close to the margins of stable cratons in the Meso-Archean.

7. Conclusion

The Pongola Supergroup of the Kaapvaal Craton in South Africa and Swaziland represents a unique assemblage of well-preserved volcanic rocks and intercalated sediments, pyroclastic rocks and sedimentary successions preserving the magmatic and sedimentary record of the oldest deposit on a stable craton. The lower, dominantly volcanic sequence of the Nsuze Group (4600 m thick in the study area) is unconformably overlain by clastic sediments of the Mozaan Group (4800 m thick). The succession is rift bounded with a suggestion of contrasting gneiss terranes on the northeast (older) and southwest (younger) sides but has no characteristics to suggest that the rocks were deposited in a rift environment. The Pongola depository may have developed along a line of weakness between crustal blocks developed at earlier times in a variety of tectonic settings.

Chemical and lithological characteristics point to plate tectonic controls for the origin of the sequence. The development of substantial (but unquantified) volumes of intermediate volcanic rocks (andesites and dacites) has similarities to continental margin and arc-like settings, although derivation by crustal contamination of mafic magmas, though unlikely on a massive scale, cannot be completely ruled out. Formation in a rifted continental environment is not supported by the lava compositions nor by the style of the volcanic and sedimentary deposits. Geochemical characteristics, such as marked depletion of Ta and Nb are signatures typical of arcs, but could also have been inherited from the crustal contamination of more primitive lavas.

Precise age determinations of intermediate volcanic rocks at the base and near the top of the Nsuze Group succession (2980 ± 10 Ma and 2968 ± 6 respectively), and close to the top of the Mozaan Group sediments (2954 ± 9 Ma) indicate a remarkably short period of deposition. While the possibility of inherited zircons cannot be ruled out, these ages allow constraints to be placed on the depositional rates with approximately 5000 m of volcanic rocks being deposited over a maximum period of 28 million years. The volcanic rocks of the upper Mozaan Group are separated from the upper part of the Nsuze Group by approximately 4000 m of sediments and equate to a maximum depositional time period of 29 million years – giving a minimum accumulation rate of 0.14 mm/yr, notwithstanding a possible time break as a result of non-deposition and development of the unconformity between these two Groups.

The oldest supracrustal volcanic sequence, the Dominion Group at the base of the Witwatersrand Supergroup in the center of the Kaapvaal Craton (Fig. 1A), has been dated at 3074 ± 6 Ma (Armstrong et al., 1991) or approximately 90 million years older than the stratigraphically lowest Nsuze Group andesite flow studied here. The correlation of the Nsuze Group in the central region with the Dominion Group is therefore unfounded. There is also little geochemical similarity, particularly for the felsic rocks and the distribution of lavas of intermediate composition, between these two occurrences, comparing with the data of Marsh et al. (1989). The only known volcanic event (the Crown Lavas) recorded in the West Rand Group of the Witwatersrand Supergroup, and which lithostratigraphically may correlate with the volcanic unit of the Mozaan Group, was dated at 2914 ± 8 Ma (Armstrong et al., 1991), a difference in age of approximately 40 million years. U–Pb ages of detrital zircons indicate that deposition of the West Rand Group commenced after 2970 Ma (Barton et al., 1989), which is consistent with the youngest age of 2968 ± 6 Ma for the underlying Nsuze Group volcanic from this work. On this basis it may be concluded that deposition of Witwatersrand Supergroup and the Mozaan Group commenced simultaneously notwithstanding the break in deposition between the Nsuze and Mozaan Groups, which may have been of limited duration.

Although conjectural at this stage, and until further studies have been carried out encompassing all facies of the Pongola basin, is it suggested that a possible analogue to recent tectonic environments for the Pongola Supergroup in the central area may have been an extensional, strike-slip controlled, continental arc basin similar to that which characterizes the southwestern United States (Busby, 2012). Features, similar to those observed in the Pongola basin, include contrasting bounding crustal blocks, evidence of rapid deposition in an extensional environment and thick sequences of sedimentary rocks and large volcanoes, wide ranges in magma compositions and variable types and styles of eruption along the length of the belt including large volume andesite eruptions of commonly highly porphyritic lavas.

The magmatic–sedimentary episode in the southeastern part of the Kaapvaal Craton ended with the emplacement of the oldest known true A-type granite stocks east and southeast of the Pongola depositary. These contain inherited zircons (cores) of effectively the same age as the youngest zircons of the Tobolsk volcanic rocks of the Mozaan Group (c. 2950 Ma) and were emplaced over the period 2837–2717 Ma. Both A1 and A2 types (Eby, 1990, 1992) are recognized concluding the final phase of stabilization of the eastern Kaapvaal Craton.

Acknowledgments

This paper is based on the M.Sc. thesis of KRY under the supervision of SBM at the University of Michigan. The project was supported by NSF grants to SBM and the South African National Research Foundation to AHW for support for the analytical work. Thanks to Kevin McKeegan for valuable assistance with the use of the Cameca IMS 1270 at the University of California – Los Angeles. Claire Palmer is thanked for assistance in the field. The following are also thanked for assistance in the field and the scientific production of this work: Noah Nhleko of the Swaziland Geological Survey, and Alex Andronikov, Charles Carrigan, Dale Austin, Stephen E. Kesler and Patricia Yocum at the University of Michigan. Comments from Axel Hofmann and an anonymous reviewer improved this paper.

Appendix A. Supplementary data

Supplementary data associated with this article can be found, in the online version, at http://dx.doi.org/10.1016/j.precamres.2012.09.015.

References

Allsopp, H.L., 1961. Rb-Sr age measurements on total rock and separated-mineral fractions from the Old Granite of the central Transvaal. Journal of Geophysical Research 66, 1499–1508.

Armstrong, N.V., Hunter, D.R., Wilson, A.H., 1982. Stratigraphy and petrology of the Archean Nsuze Group, Northern Natal and Southeastern Transvaal, South Africa. Precambrian Research 19, 75–107.

Armstrong, N.V., Wilson, A.H., Hunter, D.R., 1986. The Nsuze Group, Pongola Sequence. South Africa: geochemical evidence for Archean volcanism in a continental setting. Precambrian Research 34, 175–203.

Armstrong, R.A., Compston, W., De Wit, M.J., Williams, I.S., 1990. The stratigraphy of the 3.5–3.2 Ga Barberton greenstone belt revisited: a single zircon ion microprobe study. Earth and Planetary Science Letters 101, 90–106.

Armstrong, R.A., Compston, W., Retief, E.A., William, L.S., Welke, H.J., 1991. Zircon ion microprobe studied bearing on the age and evolution of the Witwatersrand triad. Precambrian Research 53, 243–266.

Bacon, C.R., Lanphere, M.A., 2006. Eruptive history and geochronology of Mount Mazama and the Crater Lake region, Oregon. Geological Society of America 118, 1331–1359, http://dx.doi.org/10.1130/B25906.1.

Barnes, P.M., Sutherland, R., Davy, B., Delteil, J., 2001. Rapid creation and destruction of sedimentary basins on mature strike-slip faults: an example from the offshore Alpine fault, New Zealand. Journal of Structural Geology 23, 1727–1739.

Barton, J.M., Hunter, D.R., Jackson, M.P.A., Wilson, A.C., 1983. Geochronologic and Sr-Isotopic studies of certain unit in the Barberton granite-greenstone terrane, Swaziland. Transactions of the Geological Society of South Africa 86, 71–80.

Barton, E.S., Compston, W., Williams, I.S., Bristow, J.W., Hallbauer, D.K., Smith, C., 1989. Provenance ages for the Witwatersrand Supergroup and the Ventersdorp Contact Reef: contraints from ion-microprobe U-Pb ages of detrital zircons. Economic Geology 84, 2012–2019.

Bédard, J.H., Harris, L.B., Thurston, P., 2012. The hunting of the snArc. Precambrian Research, http://dx.doi.org/10.1016/j. precamres. 2012. 04.001.

Beukes, N.J., Cairncross, B., 1991. A lithostratigraphic – sedimentological reference profile of the late Archaean Mozaan Group. Pongola Supergroup: application to sequence stratigraphy and correlation to the Witwatersrand Supergroup. South African Journal of Geology 94, 44–59.

Beukes, N.J., Lowe, D.R., 1989. Environmental control on diverse stromatolite morphologies in the 3000 Myr Pongola Supergroup, South Africa. Sedimentology 36, 383–397.

Brandl, G., Cloete, M., Anhaeuser, C.R., 2006. Archaean greenstone belts. In: Johnson, M.R., Anhaeuser, C.R., Thomas, R.J. (Eds.), The Geology of South Africa. The Geological Society of South Africa, Johannesburg and the Council for Geoscience, Pretoria, pp. 9–56.

Burger, A.J., Coertze, F.J., 1973. Radiometric age measurements on rocks from southern Africa to the end of 1971. Bulletin of the Geological Survey of South Africa 58, 46.

Burke, K.C., Kidd, W.S.F., Kusky, T.M., 1985. The Pongola structure of southeastern Africa; the world's oldest preserved rift? Journal of Geodynamics 2, 35–49.

Busby, C.J., 2004. Continental growth at convergent margins facing large ocean basins: a case study from Mesozoic Baja California, Mexico. Tectonophysics 392, 241–277.

Busby, C.J., 2012. Extensional and transtensional continental arc basins: case studies from the southwestern United States. In: Busby, C.J., Azor, A. (Eds.), Tectonics of Sedimentary Basins: Recent Advances. Blackwell Publishing Ltd., pp. 382–404.

Capdevila, R., Goodwin, A.M., Ujike, O., Gorton, M.P., 1982. Trace-element geochemistry of Archean volcanic rocks and crustal growth in southwestern Abitibi Belt, Canada. Geology 10, 418–422.

Carlson, R.W., Hunter, D.R., Barker, F., 1983. Sm-Nd age and isotopic systematics of the bimodal suite, Ancient Gneiss Complex, Swaziland, southern Africa. Nature 305, 701–704.

Choi, S.H., Mukasa, S.B., Zhou, X.-H., Xian, X.H., Andronikov, A.V., 2008. Mantle dynamics beneath East Asia constrained by Sr, Nd, Pb and Hf isotopic systematics of ultramafic xenoliths and their host basalts from Hannuoba, North China. Chemical Geology 248, 40–61.

Collins, W.J., Beams, S.D., White, A.J.R., Chappell, B.W., 1982. Nature and origin of A-type granites with particular reference to southeastern Australia. Contributions to Mineralogy and Petrology 80, 189–200.

Compston, W., Kröner, A., 1988. Multiple zircon growth within early Archaean tonalitic gneiss from the Ancient Gneiss Complex, Swaziland. Earth and Planetary Science Letters 87, 13–28.

Eby, G.N., 1990. The A-type granitoids: a review of their occurrence and chemical characteristics and speculations on their petrogenesis. Lithos 26, 115–134.

Eby, G.N., 1992. Chemical subdivision of the A-type granitoids: petrogenetic and tectonic implications. Geology 20, 641–644.

Farrow, D.J., Harmer, R.E., Hunter, D.R., Eglington, B.M., 1990. Rb-Sr and Pb-Pb dating of the Anhalt leucotonalite, northern Natal. South African Journal of Geology 93, 696–701.

Gaal, G., 1986. 2200 Million years of crustal evolution: the Baltic shield. Geological Society of Finland Bulletin 58, 149–168.

Gamble, J.A., Price, R.C., Smith, I.E.M., McIntosh, W.C., Dunbar, N.W., 2003. 40Ar/39Ar geochronology of magmatic activity, magma flux and hazards at Ruapehu volcano, Taupo volcanic zone, New Zealand. Journal of Volcanology and Geothermal Research 120, 271–287, http://dx.doi.org/10.1016/S0377-0273(02)00407-9.

Gold, D.J.C., 2006. The Pongola Supergroup. In: Johnson, M.R., Anhaeuser, C.R., Thomas, R.J. (Eds.), The Geology of South Africa. The Geological Society of South Africa, Johannesburg and the Council for Geoscience, Pretoria, pp. 135–147.

Gold, D.J.C., Von Veh, M.W., 1995. Tectonic evolution of the Late Archean Pongola-Mozaan basin, South Africa. Journal of African Earth Science 21, 203–212.

Gutzmer, J., Nhleko, N., Beukes, N.J., Pickard, A., Barley, M.E., 1999. Geochemistry and ion microprobe (SHRIMP) age of a quartz porphyry sill in the Mozaan Group of the Pongola Supergroup; implications for the Pongola and Witwatersrand supergroups. South African Journal of Geology 102, 139–146.

Hamilton, W.B., 1998. Archean magmatism and deformation were not products of plate tectonics. Precambrian Research 91, 143–179.

Hallberg, J.A., Johnston, C., Bye, S.M., 1976. The Archaean Marda Igneous Complex, Western Australia. Precambrian Research 3, 111–136.

Harrison, T.M., McKeegan, K.D., LeFort, P., 1995. Detection of inherited monazite in the Manaslu leucogranite by 208Pb/232Th ion microprobe dating: crystallization age and tectonic significance. Earth Planetary Science Letters 133, 271–282.

Hegner, E., Kröner, A., Hofmann, A.W., 1984. Age and isotope geochemistry of the Archaean Pongola and Ushushwana suites in Swaziland, southern Africa: a case for crustal contamination of mantle-derived magma. Earth and Planetary Science Letters 70, 267–279.

Hegner, E., Kröner, A., Hunt, P., 1994. A precise U-Pb zircon age for the Archaean Pongola Supergroup volcanics in Swaziland. Journal of African Earth Science 18, 339–341.

Hicks, N., Dunlevey, J.N., Liu, K.W., 2011. A new stromatolite occurrence in the Nsuze Group, Pongola Supergroup of northern KwaZulu-Natal, South Africa. South African Journal of Geology 114, 195–200.

Hildreth, W., Lanphere, M., 1994. Potassium-argon geochronology of a basalt-andesite-dacite arc system—The Mount Adams volcanic field. Cascades Range of southern Washington: Geological Society of America Bulletin 106, 1413–1429, http://dx.doi.org/10.1130/0016-7606(1994), 106<1413:PAGOAB>2.3.CO;2.

Hunter, D.R., 1957. The geology, petrology and classification of the Swaziland granites and gneisses. Transactions of the Geological Society of South Africa 60, 85–125.

Hunter, D.R., 1973. The granitic rocks of the Precambrian in Swaziland. In: Lister, L.A. (Ed.), Symposium on Granites, Gneisses and Related Rocks. Special Publication of the Geological Society of South Africa, 3, pp. 131–147.

Hunter, D.R., Allen, A.R., Millin, P., 1983. A preliminary note on Archaean supracrustal and granitoid rocks west of Piet Retief. Transactions of the Geological Society of South Africa 86, 301–306.

Hunter, D.R., Barker, F., Millard Jr., H.T., 1984. Geochemical investigation of Archean bimodal and Dwalile metamorphic suites, Ancient Gneiss Complex, Swaziland. Precambrian Research 24, 131–155.

Hunter, D.R., Wilson, A.H., 1988. A continuous record of crustal evolution from 3.5 Ga to 2.6 Ga in Swaziland and northern Natal. South African Journal of Geology 91, 57–74.

Jicha, B.R., Singer, B.S., 2006. Volcanic history and magmatic evolution of Seguam Island, Aleutian Island arc, Alaska. Geological Society of America Bulletin 118, 805–822, http://dx.doi.org/10.1130/B25861.1.

Kamo, S., Davis, D., 1991. A review of the geochronology from the Barberton Mountain Land. In: Ashwal, L.D. (Ed.), Two Cratons and an Orogen – Excursion Guidebook and Review Articles for Field Workshop through Selected Archaean Terranes of Swaziland, South Africa and Zimbabwe. IGCP Project. Department of Geology, University of the Witwatersrand, Johannesburg 280, pp. 59–68.

Kamo, S.L., Davis, D.W., 1994. Reassessment of Archean crustal development in the Barberton Mountain Land, South Africa, based on U-Pb dating. Tectonics 13, 167–192.

Kamo, S.L., Davis, D.W., De Wit, M.J., 1990. U-Pb geochronology of Archean plutonism in the Barberton region, South Africa: 800 m.y. of crustal evolution. Abstr. 7th Int. Conf. Geochron. Cosmochron. Isot. Geol. (ICOG7), 23. Geological Society of Austrralia, Canberra, p. 53.

Kent, L.E., 1980. Stratigraphy of South Africa. Part 1: Lithostratigraphy of the Republic of South Africa, South West Africa/Namibia and the Republics of Bophuthatswana, Transkei and Venda. Geological Survey South Africa Handbook, 8. South African Committee for Stratigraphy, 690 pp.

Kisters, A., Belcher, R., Poujol, M., Stevens, G., Moyen, J.-F., 2006. A 3.2 Ga magmatic arc preserving 50 Ma of crustal convergence in the Barberton terrane, South Africa. In: AGU Fall Meeting, 11-15 December 2006, San Francisco, USA.

Kröner, A., Compston, W., Williams, I.S., 1989. Growth of early Archaean crust in the Ancient Gneiss Complex of Swaziland as revealed by single zircon dating. Tectonophysics 161, 271–298.

Kröner, A., Tegtmeyer, A., 1994. Gneiss-greenstone relationships in the Ancient Gneiss Complex of southwestern Swaziland, southern Africa, and implications for early crustal evolution. Precambrian Research 67, 109–139.

Kröner, A., 2007. The Ancient Gneiss Complex of Swaziland and environs: record of early Archean crustal evolution in southern Afrca. In: Van Kranendonk, M.J., Smithies, R.H., Bennett, V.C. (Eds.), Earth's Oldest Rocks, Developments in Precambrian Geology, 15. Elsevier B.V., pp. 465–480.

Kusky, T.M., 1990. Accretion of the Archean Slave province. Geology 17, 63–67.

Layer, P.W., Kröner, A., McWilliams, M., Burghele, A., 1988. Paleomagnetism and age of the Archean Usushwana Complex, southern Africa. Journal of Geophysical Research 93, 449–457.

Loiselle, M.C., Wones, D.R., 1979. Characteristics and origin of anorogenic granites. Geological Society of America Abstracts with Programs 11, 468.

Lowe, D.R., 1999. Shallow-water sedimentation of accretionary lapilli-bearing strata of the Msauli Chert: evidence of explosive hydromagmatic komatiitic volcanism. In: Lowe, D.R., Byerly, G.R. (Eds.), Geological Evolution of the Barberton Greenstone Belt, South Africa. Special Paper 329. Geological Society of America, pp. 213–232.

Ludwig, K.R., 1999. Users Manual for Isoplot/Ex, v.2.3, A Geochronological Toolkit for Microsoft Excel, Berkeley Geochronology Center Spec. Pub. 1a, p. 52.

Maphalala, R., Kröner, A., 1993. Pb-Pb single zircon ages for the younger Archaean granitoids of Swaziland, southern Africa. In: Maphalala, R., Mabuz, M. (Eds.), Extended Abstracts 16th Colloquium of African Geology.

Marsh, J.S., Bowen, M.P., Rogers, N.W., Bowen, T.B., 1989. Volcanic rocks of the Witwatersrand Triad, South Africa II: petrogenesis of mafic and felsic rocks of the Dominion Group. Precambrian Research 44, 39–65.

Matthews, P.E., 1990. A plate tectonic model for the Late-Archaean Pongola Supergroup in southeastern Africa. In: Sychanthavong, S.P.H. (Ed.), Crustal Evolution and Orogeny. A.A. Balkema, Rotterdam, pp. 41–73.

McCourt, S., 1995. The crustal architecture of the Kaapvaal crustal block South Africa, between 3.5 and 2.0 Ga. Mineralium Deposita 30, 89–97.

McDonough, W.F., Sun, S.-s., 1995. The Composition of the Earth. Chemical Geology 10, 223–253.
McLennan, S.M., Taylor, S.R., 1981. Role of subducted sediments in island-arc magmatism: constraints from REE patterns. Earth and Planetary Science Letters 54, 423–430.
Meyer, F.M., Reimold, W.U., Walraven, F., 1993. The evolution of the Archaean granitic crust in the south-eastern Kaapvaal Craton, South Africa. Terra Abstracts 5, 319.
Moyen, J.-F., Stevens, G., Kisters, A.F.M., Belcher, R.W., 2007. TTG plutons of the Barberton terrane South Africa. In: van Kranondonk, M.J., Smithies, H., Bennett, V. (Eds.), Developments in Precambrian Geology 15. Earth's Oldest Rocks. Elsevier, Amsterdam, pp. 607–668.
Norrish, K., Hutton, J.T., 1969. An accurate spectrographic method for the analysis of geologic materials. Geochemica et Cosmochimica Acta 33, 431–454.
Nhleko, N., 2003. The Pongola Supergroup in Swaziland. Ph.D. Thesis (Unpublished). Rand Afrikaans University, Johannesburg, p. 299.
Olsson, J., 2012. U-Pb baddeleyite geochronology of Precambrian mafic dyke swarms and complexes in southern Africa – regional extensional events and the origin of the Bushveld Complex. Litholund thesis no. 22. Lund University, Sweden.
Paces, J.B., Miller Jr., J.D., 1993. Precise U-Pb ages of Duluth Complex and related mafic intrusions, northeastern Minnesota; geochronological insights to physical, petrogenetic, paleomagnetic, and tectonomagnetic processes associated with the 1.1 Ga Midcontinent Rift System. Journal of Geophysical Research 98 (13), 13 997–14 013.
Pearce, J.A., 2008. Geochemical fingerprinting of oceanic basalts with applications to ophiolite classification and the search for Archean oceanic crust. Lithos 100, 14–48.
Plank, T., 2005. Constraints from thorium/lanthanum on sediment recycling at subduction zones and the evolution of the continents. Journal of Petrology 46, 921–944.
Quidelleur, X., Grove, M., Lovera, O.M., Harrison, T.M., Yin, A., Ryerson, F.J., 1997. Thermal evolution and slip history of the Renbu Zedong Thurust, southeastern Tibet. Journal of Geophysical Research 102, 2659–2679.
Saha, L., Hofmann, A., Xie, H., Hegner, E., Wilson, A., Wan, Y., Liu, D., Kröner, A., 2010. Zircon ages and metamorphic evolution of the Archean Assegaai – De Kraalen granitoid – greenstone terrane, southeastern Kaapvaal Craton. American Journal of Science 310, 1384–1420, Alfred Kröner Special Issue: Part II.
Schoene, B., de Wit, M.J., Bowring, S.A., 2008. Meso-archean assembly and stabilization of the eastern Kaapvaal craton: A structural – thermochronological perspective. Tectonics 27, TC5010, http://dx.doi.org/10.1029/2008TC002267.
Schoene, B., Bowring, S.A., 2010. Rates and mechanisms of Mesoarchean magmatic arc contruction, eastern Kaapvaal craton, Swaziland. Geological Society of America Bulletin 122, 408–429.
Singer, B.S., Jicha, B.R., Harper, M.A., Naranjo, J.A., Lara, L.E., Morena-Roa, H., 2008. Eruptive history, geochronology, and magmatic evolution of the Puyehue-Cordón Caulle volcanic complex, Chile. Geological Society of America Bulletin 120, 599–618, http://dx.doi.org/10.1130/B26276.1.
Smithies, R.H., Champion, D.C., Van Kranendonk, M.J., 2007. The oldest well-preserved felsic volcanic rocks on Earth: geochemical clues to the early evolution of the Pilbara Supergroup and implications for the growth of a paleoarchean protocontinent. In: Van Kranendonk, M.J., Smithies, R.H., Bennett, V.C. (Eds.), Earth's Oldest Rocks, Developments in Precambrian Geology, 15. Elsevier B. V., pp. 339–367.
South African Geological Survey, 1988. 1:250,000 Series Geological Map of Vryheid (2730).
Stevens, G., Moyen, J.-F., 2007. Metamorphism in the Barberton granite greenstone terrane: a record of Paleoarchean accretion. In: Van Kranendonk, M.J., Smithies, R.H., Bennett, V.C. (Eds.), Earth's Oldest Rocks, Developments in Precambrian Geology, 15. Elsevier B. V., pp. 669–698.
Sylvester, P.J., Attoh, K., Schulz, K.J., 1987. Tectonic study of late Archean bimodal volcanism in the Michipicoten (Wawa) Greenstone Belt, Ontario. Canadian Journal of Earth Science 24, 1120–1134.
Tankard, A.J., Jackson, M.P.A., Eriksson, K.A., Hobday, O.K., Hunter, D.R., Minter, W.E.L., 1982. Crustal Evolution of Southern Africa. Springer – Verlag, New York, p. 523.
Thurston, P.C., 1994. Archean volcanic patterns. In: Condie, K.C. (Ed.), Archean Crustal Evolution. Elsevier, Amsterdam, p. 542.
Van Kranendonk, M.J., Smithies, R.H., Hickman, A.H., Champion, D.C., 2007. Paleoarchean development of a continental nucleus: the east Pilbara terrane of the Pilbara craton, western Australia. In: Van Kranendonk, M.J., Smithies, R.H., Bennett, V.C. (Eds.), Earth's Oldest Rocks, Developments in Precambrian Geology, 15. Elsevier B. V., pp. 307–337.
Von Brunn, V., Hobday, D.K., 1976. Early Precambrian tidal sedimentation in the Pongola Supergroup of South Africa. Journal of Sedimentary Petrology 46, 670–679.
Walraven, F., Pape, J., 1994. Pb-Pb whole-rock ages for the Pongola Supergroup and the Usushwana Complex, South Africa. Journal of African Earth Science 18, 297–308.
Wiedenbeck, M., Allé, P., Corfu, F., Griffin, W.L., Meier, M., Oberli, F., Von Quadt, A., Roddick, J.C., Spiegel, W., 1995. Three natural zircon standards for U-Th-Pb, Lu-Hf, trace element and REE analyses. Geostandards Newsletter 19, 1–23.
Wilson, A.C., 1982. Geologic Map of Swaziland. Government of Swaziland.
Wilson, A.H., Carlson, R.W., 1989. A Sm-Nd and Pb-Pb isotopic study of Archaean greenstone belts in the southern Kaapvaal Craton, South Africa. Earth and Planetary Science Letters 96, 89–105.
Wilson, A.H., 2003. A new class of silica enriched, highly depleted komatiites in the southern Kaapvaal Craton, South Africa. Precambrian Research 127, 125–141.
Wilson, A.H., Grant, C.E., 2006. Physical volcanology and compositions of the basaltic lavas in the Archaean Nsuze Group, White Mfolozi inlier, South Africa. In: Reimold, W.U., Gibson, R.L. (Eds.), Processes on the Early Earth. Geological Society of America Special Paper 405. , pp. 255–289.
Wronkiewicz, D.J., Condie, K.C., 1989. Geochemistry and provenance of sediments from the Pongola Supergroup, South Africa; evidence for a 3.0-Ga-old continental craton. Geochemica et Cosmochimica Acta 53, 1537–1549.
Xie, H.Q., Hofmann, A., Wan, Y.S., Saha, L., Kröner, A., Liu, D.Y., 2010. 3.2 Ga metamorphic event in the Paulpietersburg area, South Africa, and tectonic implications. In: Excursion Guidebook and Abstract Volume, Field Workshop, Early Crustal Evolution of the Southeastern Kaapvaal Craton in South Africa and Swaziland, 17-23 May 2010, Paulpietersburg/Badplaas, South Africa and Ezulwini, Swaziland, p. 98.
Xie, H., Hofmann, A., Hegner, E., Wilson, A.H., Wan, Y., Liu, D., 2012. Zircon SHRIMP dating confirms a Palaeoarchaean supracrustal terrain in the southeastern Kaapvaal Craton, South Africa. Gondwana Research 21, 818–828.